MICROCOPY RESOLUTION TEST CHART

NATIONAL BUREAU OF STANDARDS – 1963 – A

10

AD-A166 772

TYPHOON STRUCTURAL VARIABILITY

BY

CANDIS L. WEATHERFORD

P.I. WILLIAM M. GRAY

COLORADO STATE UNIVERSITY
1870
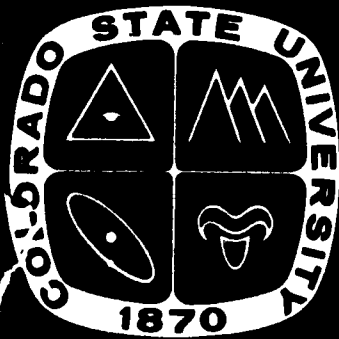
REPORT DOCUMENTATION PAGE		READ INSTRUCTIONS BEFORE COMPLETING FORM
1. REPORT NUMBER AFIT/CI/NR 86- 10T	2. GOVT ACCESSION NO. AD A 166 272	3. RECIPIENT'S CATALOG NUMBER
4. TITLE *(and Subtitle)* Typhoon Structural Vairability		5. TYPE OF REPORT & PERIOD COVERED THESIS/DISSERTATION
		6. PERFORMING ORG. REPORT NUMBER
7. AUTHOR(s) Candis L. Weatherford		8. CONTRACT OR GRANT NUMBER(s)
9. PERFORMING ORGANIZATION NAME AND ADDRESS AFIT STUDENT AT: Colorado State Univ		10. PROGRAM ELEMENT, PROJECT, TASK AREA & WORK UNIT NUMBERS
11. CONTROLLING OFFICE NAME AND ADDRESS AFIT/NR WPAFB OH 45433-6583		12. REPORT DATE 1985
		13. NUMBER OF PAGES 77+
14. MONITORING AGENCY NAME & ADDRESS*(if different from Controlling Office)*		15. SECURITY CLASS. *(of this report)* UNCLASS
		15a. DECLASSIFICATION/DOWNGRADING SCHEDULE

16. DISTRIBUTION STATEMENT *(of this Report)*

APPROVED FOR PUBLIC RELEASE; DISTRIBUTION UNLIMITED

17. DISTRIBUTION STATEMENT *(of the abstract entered in Block 20, if different from Report)*

18. SUPPLEMENTARY NOTES
APPROVED FOR PUBLIC RELEASE: IAW AFR 190-1

LYNN E. WOLAVER
Dean for Research and
Professional Development
AFIT/NR, WPAFB OH 45433-6583

19. KEY WORDS *(Continue on reverse side if necessary and identify by block number)*

20. ABSTRACT *(Continue on reverse side if necessary and identify by block number)*

DTIC
SELECTED
APR 1 0 1986
E

DD FORM 1473 EDITION OF 1 NOV 65 IS OBSOLETE
1 JAN 73

TYPHOON STRUCTURAL VARIABILITY

By

Candis L. Weatherford

Department of Atmospheric Science

Colorado State University

Fort Collins, Colorado 80523

October, 1985

Department of Atmospheric Science Paper No. 391

QUALITY INSPECTED 3

ABSTRACT

This paper describes the varying structure of the tropical cyclone wind profile in terms of its core intensity, outer strength, and size where core intensity is defined by the tropical cyclone's minimum central sea-level pressure, outer strength is an average tangential wind speed from 60 to 150 n mi (111-278 km), and size measures the radial extent of 30-kt and 50-kt surface winds. Analysis was performed on 700 mb aircraft data from over 500 reconnaissance missions into 66 tropical cyclones of the northwestern Pacific. All these cyclones were of typhoon intensity ($V_{max} \geq 65$ knots) sometime during their lifecycle. This data set is uniquely suited to fill the dual needs of: 1) providing inner wind profile information out to 4° radius, thus allowing the cyclone's strength to be measured, and 2) being able to sample the entire life cycle of the tropical cyclone from depression through supertyphoon stages. The focus of this study is on the outer strength region.

The reasons for the focus on cyclone outer strength are twofold. First, in order to meet very immediate operational needs, the forecaster must be able to predict the low-level wind profile and where it crosses gale and hurricane force wind speeds, no matter what the core intensity of the tropical cyclone. Second, the theoretician must understand the surrounding wind flow in order to better model storm surge, total rainfall, and the effects on core intensification that inertial stability plays. A depiction of outer strength is essential.

Cyclone strength is compared to the adjoining regions of the wind profile of intensity and the 30-kt domain. Results show that outer strength and core intensity vary greatly with each other while outer strength and the 30-kt wind domain appear closely correlated. However, if information is available on the size of the eye, much of the variance between core intensity and outer strength can be reduced. Outer strength is also stratified by latitude, season, time of day, and cyclone motion. Finally, typical tangential wind profiles are provided for core intensities ranging from the tropical storm to the supertyphoon.

FOREWORD

by William M. Gray

Regular reconnaissance flights into typhoons and tropical cyclones in the western Pacific have been conducted by the United States military since the end of World War II. So far this flight information has been used almost excusively in an operational sense to track the centers of these storms and to measure how intense they are. Almost no research has been accomplished on this most extensive, unique, and valuable flight information. A large gap exists in our measurement of the tropical cyclone from 1° radius (where Atlantic research flights have typically terminated) to $2-3^{\circ}$ radius (where composites of rawinsondes become dense and more reliable).

The measurement capability of the military reconnaissance aircraft into tropical storms has improved over the years. This was particularly the case after the development and installation of Doppler wind navigation equipment on western Pacific military aircraft in the late 1960's. Also, beginning in the middle 1970's, systematic flight patterns were instituted in which four radial legs were flown in and out of the tropical cyclone in equally spaced azimuthal segments to 150 n mi (~278 km) with two of these flight legs extending out to 250 n mi (~463 km). These systematic flight tracks are made nearly every tweleve hours on nearly every tropical cyclone in the west Pacific. This operational reconnaissance flight data offers much potential for increased knowledge about tropical cyclones because of the twice-a-day time continuity of

flight data on most cyclones from genesis stage to extratropical

transition and the large areal coverage of each flight mission. It is

likely that much new knowledge about the tropical cyclone will be

forthcoming from a careful examination of this flight data.

It is surprising that so little research has so far been

accomplished on this flight data. The potentials and hindrances in

performing research on this flight data were summarized by myself - Gray

(1978) - in a report to the World Meteorological Organization (WMO).

> No greater loss of opportunity for tropical cyclone
> research and general knowledge gain is more evident than
> that of the US military and civilian meteorological
> community in its failure to exploit its unique tropical
> cyclone research opportunities on Guam. Extensive
> typhoon aircraft reconnaissance has been going on since
> the end of World War II at the cost of tens' of millions
> of dollars per year. The knowledge gained from these
> flights has been ever so much less than it could have
> been because almost no follow-up research on this data
> has been accomplished. Long-term military
> duty assignments on Guam have not been permitted. The
> US military system of 2-year rotation back to state-
> side duty assignments not related to typhoons and the
> required military concentration on the operational
> mission alone has not been advantageous for research
> being accomplished by the military itself.

One of the many problems with using this reconnaissance data for

research has been the difficulty that non-military personnel have in

performing adequate data reduction from a data set that is not set up

for research; e.g., data is not provided in storm relative coordinates,

and changes to the code occur nearly twice a year. It has been

difficult to keep up with all of these changes in codes and flight

missions and the other problems encountered in sampling these storms.

It is important that this data be worked on by researchers who has spent

time making these reconnaissance flights. Unfortunately the Guam

iv

reconnaissance officers rarely follow up their unique operational experiences with research on the flight data they have taken. The research reported in this paper tries to break this practice. The author was a weather reconnaissance officer with the 54th Weather Reconnaissance Squadron out of Andersen Air Force Base, Guam, for the years 1980 through 1982. She has flown into approximately 35 different tropical cyclones and made approximately 90 individual flights during this 3-year period. She left Guam in late 1982 and then started an immediate study and data reduction of this flight data. This involved a trip to the National Climatic Center in Asheville, NC, to xerox all this flight data.

This paper is a result of the curiosity generated by the author during her typhoon flight missions from Guam during these years and the tropical cyclone research environment with which she has been associated at Colorado State University.

TABLE OF CONTENTS

LIST OF DEFINITIONS AND ACRONYMS

CYCLONE: Tropical cyclone from tropical depression to supertyphoon intensity.

INTENSITY: Minimum sea-level pressure of the cyclone (SLP_{min}), measured in whole millibars (mb). Core intensity referred to simply as "intensity".

JTWC: Joint Typhoon Warning Center (U.S. Air Force and Navy) based on Guam.

MOT: Coordinate system relative to the moving tropical cyclone center (Motion).

NAT: Coordinate system relative to the tropical cyclone center with the center held fixed (Natural).

R-30:   Average radius of the 30-kt surface wind domain (35 kt at 700 mb).

R-50   Average radius of the 50-kt surface wind domain (59 kt at 700 mb).

STRENGTH: Time and area-weighted average tangential wind speed relative to the moving cyclone using four flight legs within a range of 60 to 150 n mi taken over a 12-hour period. Outer strength referred to simply as "strength".

1. INTRODUCTION

The research presented here focused on two major goals: 1) to explore the extent to which these flight data could be used for research purposes that could lead to increased insights into the structure of northwestern Pacific tropical cyclones; and 2) to attempt to quantitatively measure the variability of structure from genesis to extratropical transition and from cyclone to cyclone. This research primarily concentrated on the tropical cyclone's surrounding wind data (termed 'strength' or outer strength) and how this surrounding wind circulation and its changes are related to the cyclone's central pressure. For instance, do cyclones strengthen and intensify simultaneously? The association of cyclone core intensity with outer 50- and 30-kt wind radii will be presented in this paper, as will the relationship of the eye's size to the cyclone's outer wind profile.

1.1 Background

The complete wind profile of the tropical cyclone from its center to large radii has generally not been studied. Portions of it have received great attention, particularly inside 1° and outside 3° latitude radius. However, the part that lies between the center and the outer region has gone relatively unstudied - see Fig. 1.1. This region is here referred to as outer strength. Yet, the importance of outer strength is to provide added insight into studies of storm surges, heavy rainfall, the inertial stability of the cyclone vortex, and the structure of the wind profile. Therefore, this study has attempted to
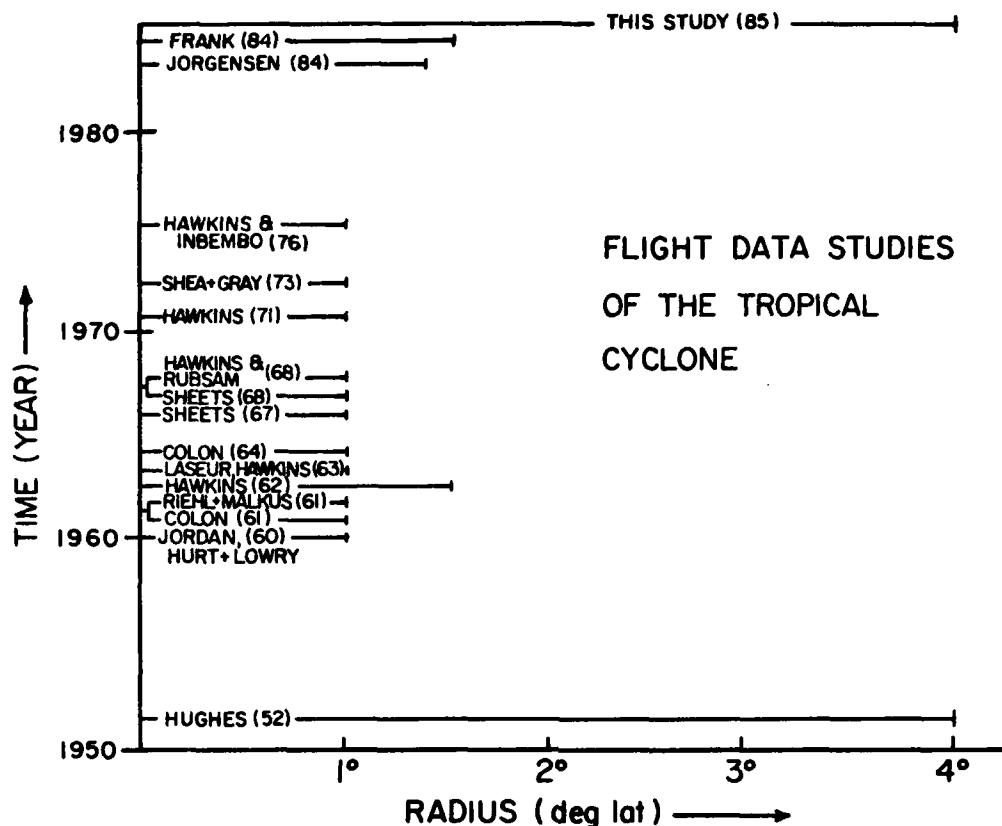
Fig. 1.1. Past flight data studies of the tropical cyclone. Research flights have focused on the inner 1° of the tropical cyclone and composites of rawinsondes have treated the region outside of 2-3° radius. There is a relatively data-void region in between.

fill in the present gap of tropical cyclone knowledge by focusing on strength, its deviations from the mean, its relationship to intensity and size and its role under differing seasons, times of day, cyclone directions and speeds, and latitudes.

The portion of the tropical cyclone most thoroughly studied by flight data is the section which lies inside a radius of 1°, accomplished primarily by the Hurricane Research Division, HRD, (formerly the National Hurricane Research Laboratory) during the past 30 years. In this region, most research has focused on case studies of various Atlantic hurricanes: Daisy and Helene (Riehl and Malkus, 1961; Colon, 1961, 1964); Cleo (LaSeur and Hawkins, 1963); Ella, Janice, and

Dora (Sheets, 1967, 1968); Debbie and Hilda (Hawkins, 1968, 1971); and

Allen, David, Anita and Frederick (Jorgensen, 1984). In order to obtain

an average view of the inner hurricane wind structure, Shea and Gray

(1973), Gray and Shea (1973), and Gray (1962, 1965, 1967) have performed

many multiple case and composite studies of the Atlantic inner 1° radius

region. Because of the lack of outer radius information these studies

on Atlantic hurricanes could not treat the question of outer wind

strength.

Outside 1° radius, flight data studies have been scarce. Hughes

(1952) averaged the wind profiles from 13 late 1940's large and mature

typhoons to give an average low-level view of the energetics of the

typhoon from the center to 4.5° latitude. However, the state-of-the-art

in wind measuring equipment had yet to reach a stage of reliable

accuracy as Hughes used visual estimates only of the sea state for wind

values which provided a $\pm$ 15 kt error. Besides Hughes's study,

rawinsondes have added to our knowledge of tropical cyclone structure.

Yet, composites of this source of data cannot, in general, properly

handle the region of cyclone strength due to the scarcity of upper air

reports inside $2-3^\circ$ from the center (Frank, 1977; Izawa, 1964; Miller,

1958). Still, the compositing technique sometimes has the capability to

gauge the radius of 30 kt surface winds (Frank and Gray, 1980). Merrill

(1984) used synoptic analyses to glean radii of outer closed isobars and

found no significant correlation of this size measure with core

intensity.

With the help of the northwestern Pacific aircraft data, it is

hoped that this void of knowledge between the inner region aircraft

studies and the outer rawinsonde work can be filled. Many questions are

waiting to be answered. How do the winds in the outer strength region relate to the maximum winds? How does the entire radial wind profile from the center to 4° change as the system intensifies or as it fills? What are the extremes in outer strength which a cyclone can attain? How might outer strength be related to season, latitude, time of day or cyclone motion? What are typical wind profiles for all stages of intensity from tropical storm to supertyphoo.?

In order to address these questions, over 500 flight missions into 66 tropical cyclones of the northwestern Pacific were analyzed from the cyclone center to 250 n mi, thereby sensing the system from the center through the strength region out to the extent of 30 kt. All these 66 tropical cyclones were of typhoon intensity ($V_{max} \geq 65$ knots) sometime during their lifetime. Chapter 2 explains the handling of this data from its raw form to a mean wind profile representative of each flight mission. Chapter 3 provides a climatological picture of the wind profile by month, latitude, cyclone motion and time of day. Chapter 4 deals with the interaction between the intensity of the cyclone and its measured strength. Outer strength is further compared with the domain of 30-kt winds. Chapter 5 incorporates the relationship that an eye has on the entire wind profile.

2. THE DATA SET

US Air Force WC-130 aircraft were routinely flown into tropical cyclones in the northwestern Pacific strictly to meet the operational needs of the Joint Typhoon Warning Center (JTWC) for the period 1980-1982. These flight missions were usually conducted twice a day into tropical cyclones during their entire lifetime. This data set was thus broken down into 12-hour periods of the day to match the typical times of the flight missions. In this study, all the data were obtained at the 700 mb pressure level, believed to be representative of the lower half of the troposphere. Because the typical flight pattern of this data set extended nearly four times as far out from the cyclone center as most previous flight data studies, data processing involved maximizing on this additional data, adjusting it to a cyclone-relative coordinate system and constructing a representative wind profile for each flight.

2.1 The Typical Flight Pattern

Each flight began with an inward penetration track from 250 n mi (463 km) radius from the estimated cyclone center followed by a 4-radial leg cloverleaf pattern inside the 150 n mi (278 km) radius as depicted in Fig. 2.1. Observations of wind, height of 700 mb surface, temperature, and dew point were taken every 30 n mi. This standardized flight track allowed comparisons of flight data between cyclones or between different time periods of one cyclone.

TYPICAL FLIGHT PATTERN
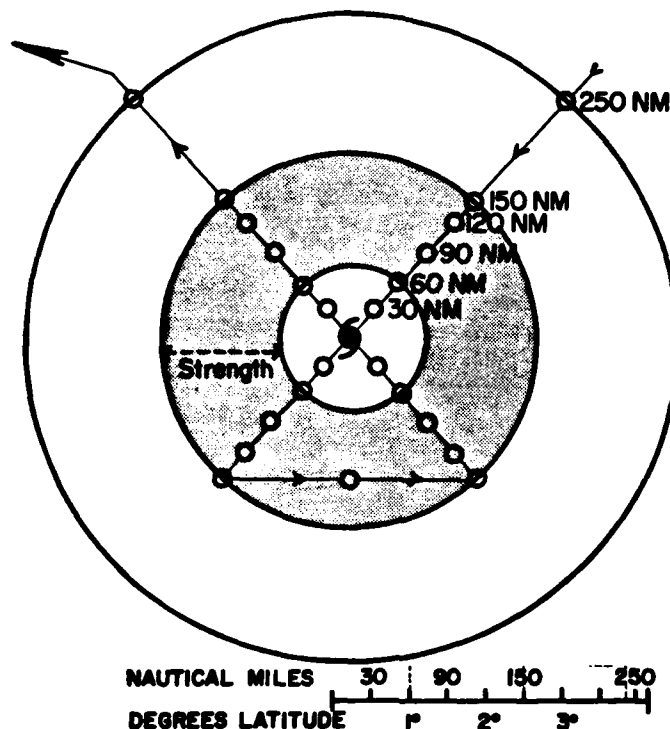## 700 mb LEVEL 2-FIX

Fig. 2.1. Typical 700 mb flight pattern - range marks denote required
          observation points (stippled area encloses 'strength').

Henderson (1978) has extensively discussed the meteorological
measuring equipment on board the WC-130. Of interest in this study were
the radar, navigational equipment and doppler wind equipment.
Measurements of the eye were obtained from 3 cm radar while navigation
relied on the LORAN and Omega equipment. The Doppler wind equipment had
two sources of error:

1. It registered signals relative to the position of the sea
   below. A moving sea under the stress of the wind will act to
   underestimate the real flight level wind speed by about 5 to 8
   percent (Grocott, 1963).

2. The Doppler signal was occasionally attenuated by heavy rain.
   This disrupts the wind measurement.

Both of these effects were most pronounced in the eyewall. The

attenuating influence did not occur very frequently, but often enough to cause some doubt on the values of the maximum wind and radius-of-maximum-wind measurements. On the other hand, minimum sea-level pressure was measured very reliably. For these reasons, minimum sea-level pressure was used as the measure of intensity over the maximum wind measurement.

This data set is comprised of over 500 flight missions on 337 days into 66 tropical cyclones during the 3-year period of 1980-82. This period was chosen because these were the years the author flew as a reconnaissance officer. Being thus familiar with all of the flight procedures, the reconnaissance codes, their various changes and the typical sources of measuring and recording errors, compilation of the data set could be accomplished more thoroughly.

2.2 Compiling the Data

Data compilation involved reorganizing the raw data into one common data set and carefully sorting for possible recording and instrumental errors. Knowledge of the code changes was crucial. For example, during this 3-year period, five formats were used, each with a different code. It was essential to know which positions were coded to the nearest degree or nearest nautical mile, how the wind was coded when in 3, 4, or 5 digits and where and how the typical recording errors were made. All data that included any remark denoting some inconsistency were sorted out and deleted. Any other suspicious appearing data was also deleted.

2.3 Data Navigation

The average speed of motion of a tropical cyclone for this data set in the northwestern Pacific was 11 kt. Data navigation relative to a moving cyclone (MOT) was thus important. In constructing the mean outer

wind velocities that occured over the 3-4 hour period of the 4-leg
penetrations, it was necessary to position each observation relative to
the center of the cyclone at the time the observation was taken. These
center positions changed with each observation. Therefore, the problem
of navigation involved finding the most accurate source of center fixes
and interpolating these fixes in time so that each observation could be
positioned relative to the center.

In order to obtain the most accurate source of cyclone center
positions from which to interpolate the position of the continuously
moving center, a rectification was made between two sources of center
fixes. The Guam-based Joint Typhoon Warning Center (JTWC) provides 6-
hourly positions of the surface cyclone center every six hours of the
cyclone's life. These are called the 'Best Track' positions. These
post-cyclone 'Best Track' positions were derived from an analysis of
aircraft-measured centers, satellite-observed centers, land-based radar
observations, and synoptic reports. Although the 'Best Track' file
provides good continuity of positions, its center positions, on the
average, varied from the actual aircraft's 700 mb measured centers by 15
n mi, very likely due to the different levels used, navigational errors
and normal oscillations in the path of the cyclone (Annual Tropical
Cyclone Reports, 1980-1982; Holland, 1983). Use of the 'Best Track'
alone would have caused discrepancies among the center positions that
the aircraft was measuring, possibly placing the aircraft-observed
maximum winds too near the center or on the wrong side of the center.
This would have seriously affected the interpretation of the inner wind
measurements. It was determined that the best procedure to solve this
problem would be the incorporation of both the 'Best Track' and

aircraft-fixed positions in combination. The compromise involved
starting with the 'Best Track' center fixes to provide good continuity
on the speed and direction of motion of the cyclone center. Akima's
(1970) five center-point interpolation scheme was used to provide
continuous positions between the six-hourly center fixes provided by
JTWC. Akima's routine best depicted changes in cyclone direction and
speed, providing gradual, rather than abrupt turns and accelerations,
and handled looping motion quite well. Secondly, when the 'Best Track'
(as shown in Fig. 2.2) varied from an aircraft measured center, the
'Best Track' was shifted so as to pass through the exact point in space
and time of the aircraft fix. Thus, critical close-in winds, the outer
radius beginning and endpoint winds, and all data in between could be
appropriately navigated relative to the moving cyclone center as
determined by the Akima scheme. The 'Best Track' and flight center
fixes were mutually adjusted in this way so that no interior wind would
disagree with the common center position.

THE MOVING CENTER

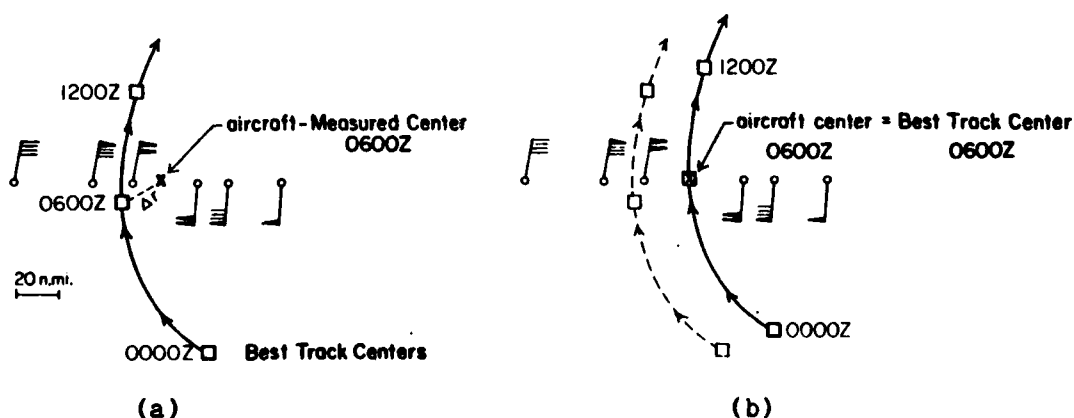(a)   (b)

Fig. 2.2.   Center fix adjustment made to navigate data positions. (a)
'Best-Track' centers provide continuous center positions but
may deviate from aircraft measured center, (b) 'Best-Track'
path is shifted over to pass through aircraft measured center
in order to compensate for the discrepancy.

2.4 Constructing the Wind Profile

Since the spatial resolution of flight observations in these northwestern Pacific cyclones was much less than that in Atlantic cyclones, it was necessary to average all the radial leg flights together to obtain a representative wind profile. All tangential wind profiles were adjusted to a moving cyclone center (the MOTion coordinate abbreviated MOT). For example, Fig. 2.3 portrays the tangential wind profile of Typhoon Bill with respect to the center in both the fixed, or NATural coordinate (NAT system) – top diagram, and the relative motion coordinate system (or MOT system) – bottom diagram. Note how the large scatter of wind speeds in the NAT system has been reduced in the MOT system.

A curve-fitting routine was chosen to best depict the wind profiles in a least-squares manner. The routine used – seen in Fig. 2.3 – was
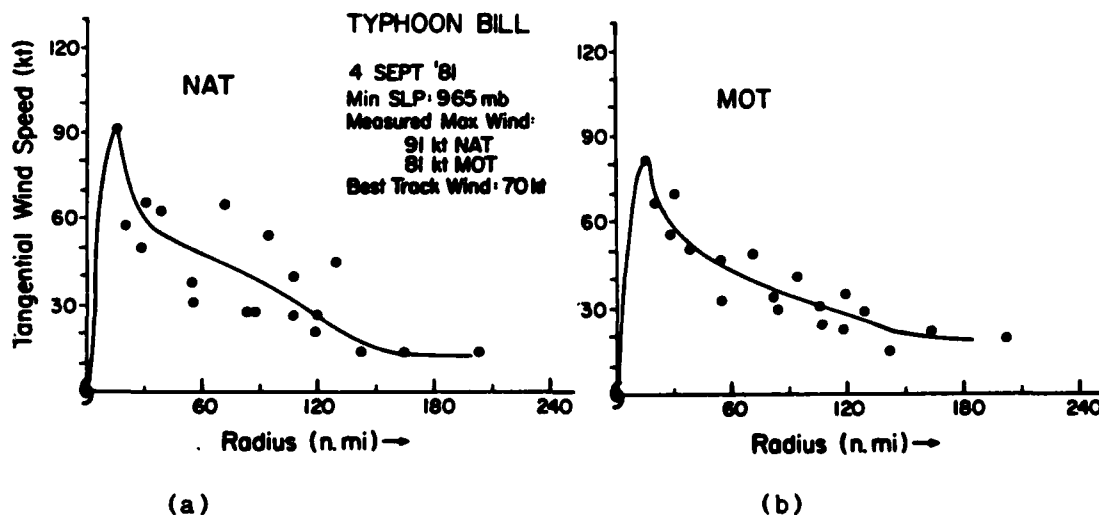

Fig. 2.3. Depiction of the wind profile of Typhoon Bill in two
coordinate systems a) natural wind speed (NAT), and b)
relative wind speed (MOT) showing the reduced scatter of wind
speeds when relative to the moving cyclone center.

called MONDER by its originators Fritsch, Carlson and Butland (1980).
This smoothing scheme calculated radial averages at 30 n mi intervals,
matching the observational frequency. No curve was drawn through a
section containing fewer than two points of data. Furthermore, the
MONDER curve routine computes 40 radial slopes and radial derivatives
between these points through a piecewise cubic-spline interpolation.
This provided smooth curves. Because the maximum wind was sometimes not
well sampled, the smoothing scheme was programmed to draw to the maximum
wind during an individual flight mission, not an average of maxima for
each leg. As previously discussed, the maximum winds along many of the
flight legs were not properly sensed and was therefore often an
underestimate.

2.5 Wind Profile Measurements

A new idea coming out of this and other studies of the CSU research
team in the last few years is the concept of distinguishing between
tropical cyclone 'intensity', which is a measure of a tropical cyclone's
central pressure (or maximum sustained low level wind), and that of
tropical cyclone 'strength', which is a measure of the surrounding wind
flow (Holland and Merrill, 1984). Figure 2.4 depicts this concept along
with various measures of size. Cyclone intensity and strength were
measured as follows:

a) CYCLONE INTENSITY - the central pressure or height of standard
    surface of the cyclone as measured at the surface or at the
    700 mb level, respectively.

Intensity is normally thought of as the maximum wind of the
cyclone. However, as previously discussed, wind intensity was not
always a consistent measure so the central height at the flight level of
700 mb or the SLP_{min} was used. While SLP_{min} was used operationally as
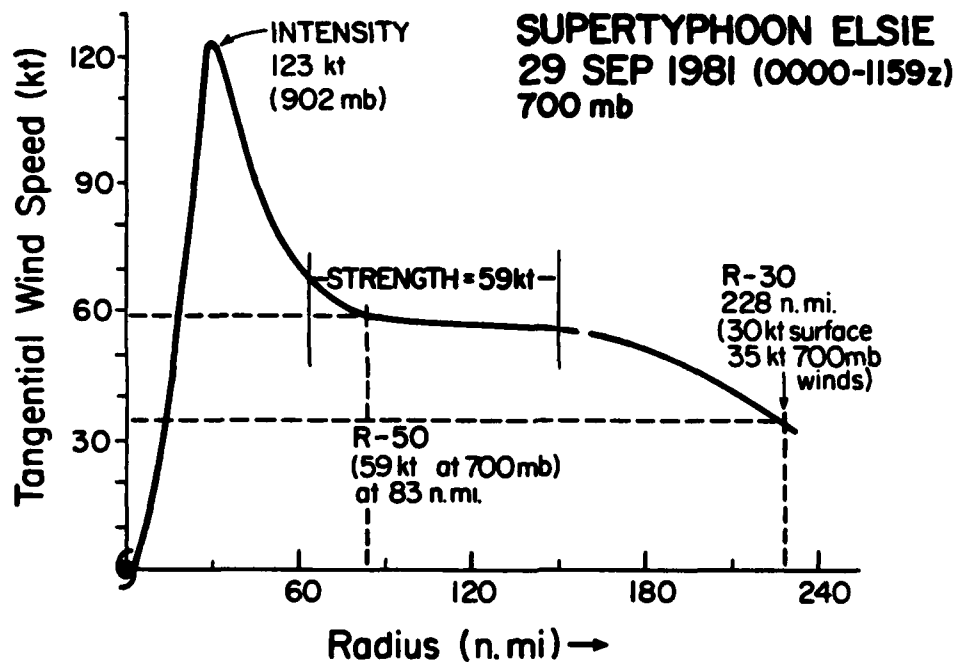
Fig. 2.4.   Intensity, strength, and size (R-30 and R-50) as distinct features along Supertyphoon Elsie's wind profile.
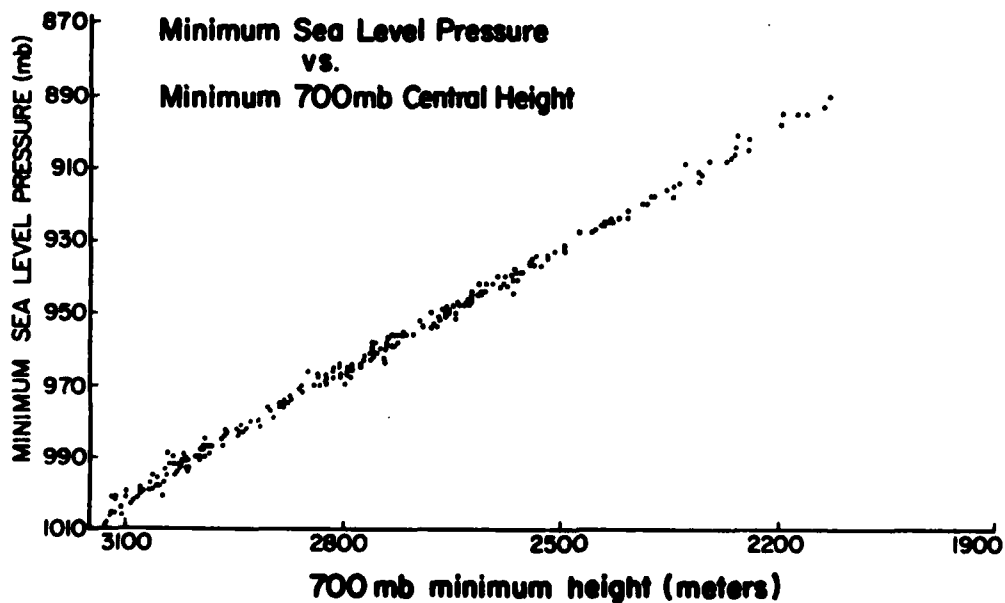

Fig. 2.5.   Scatter plot of central sea-level pressures vs. 700 mb minimum height correlating at .997.

the intensity measurement, due of the cost of the individual dropsondes it was less frequently measured than the minimum height of the 700 mb flight level. But as Fig. 2.5 shows, 700 mb height is a very good measure of the minimum sea-level pressure. The two parameters correlate at .997. This not only shows a powerful relationship of pressure changes at different levels in the center, but also that the two independent measurements were both very accurate. Thus, both the minimum 700 mb height, as converted to SLP_{min}, and the measured minimum sea-level pressure were used in this study to estimate the intensity of the cyclone.

    b) CYCLONE STRENGTH - an area-weighted average tangential
       wind speed from 60 n mi (111 km) to 150 n mi (278 km)
       in a cyclone relative motion coordinate system. Each
       flight mission normally produced one measurement of
       cyclone strength over a 12-hour period.

Cyclone strength measurements allowed comparisons of wind speeds away from, but adjoining, the maximum wind region of the cyclone. Figure 2.6 depicts examples of two radial wind profiles whose strengths are equivalent (28 kt) but whose intensities are quite different (SLP_{min} of 895 mb vs. 971 mb).

2.6 Surface Wind Estimates

Although wind data were not measured at the surface, 700 mb level winds could be used to approximate surface wind speeds. Vertical wind profile studies of winds between buoy-obtained surface winds and flight level winds by Powell (1982), flight level studies by Shea and Gray (1973) and Jorgensen (1984) and rawinsonde studies by Frank (1977) and Frank and Gray (1980) indicate that surface wind speeds are approximately 85% of the 700 mb level winds. Applying this estimate,
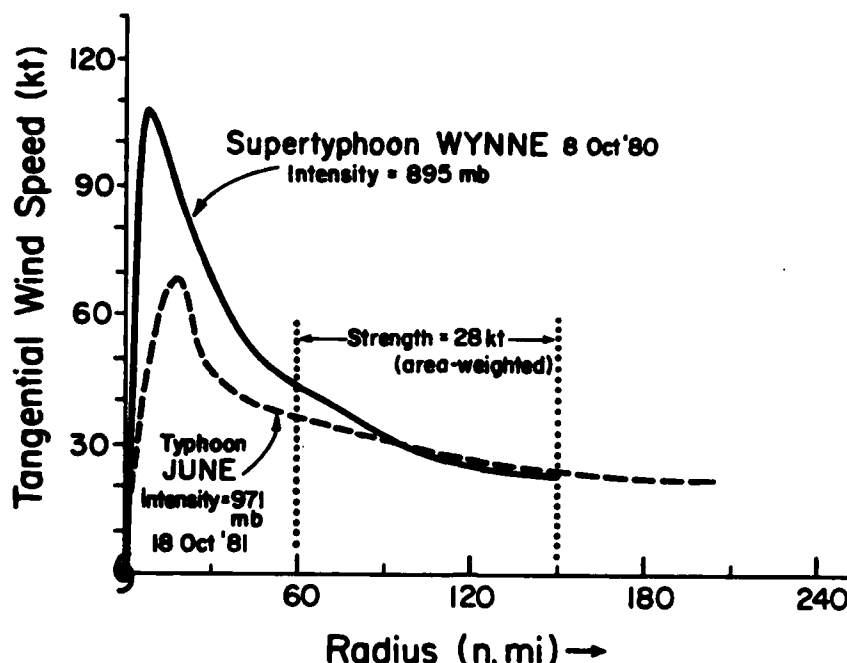
Fig. 2.6. Two examples of wind profiles whose strength values are the same for both Supertyphoon Wynne and minimal Typhoon June.

measurements of the size of 30-kt and 50-kt surface winds were obtained

using 35-kt and 59-kt flight level winds, respectively.

a) <u>R-30</u> - the average radius from the cyclone center to the 30-kt suface wind speed.

Knowledge of R-30 is an operational requirement for the JTWC

warnings. The radius of 30-kt surface winds could vary from near the

center for weak systems to beyond the 250 n mi range of this flight data

set. This meant that a four quadrant average for R-30 was obtained if

R-30 lay inside 150 n mi and a two quadrant average was used for R-30

from 150 to 250 n mi as matched the typical flight pattern (refer to

Fig. 2.1). R-30 was unavailable when:

1) the entire wind profile was greater than 30 kt (Fig. 2.7) (implying that the size is larger than the 250 n mi boundary of the flight data),

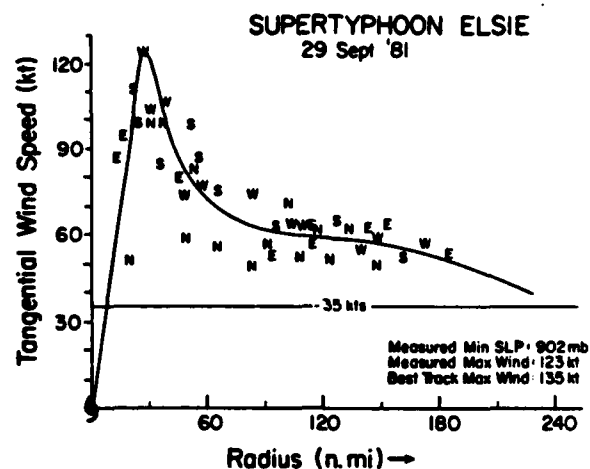2) the cyclone was a tropical depression that never attained 30 kt (Fig. 2.8), or

SUPERTYPHOON ELSIE
29 Sept '81

Measured Min SLP: 902 mb
Measured Max Wind: 123 kt
Best Track Max Wind: 135 kt

Fig. 2.7. Supertyphoon Elsie's profile is too large to measure R-30 inside the flight track region. (N = north, E = east, S = south, W = west.)
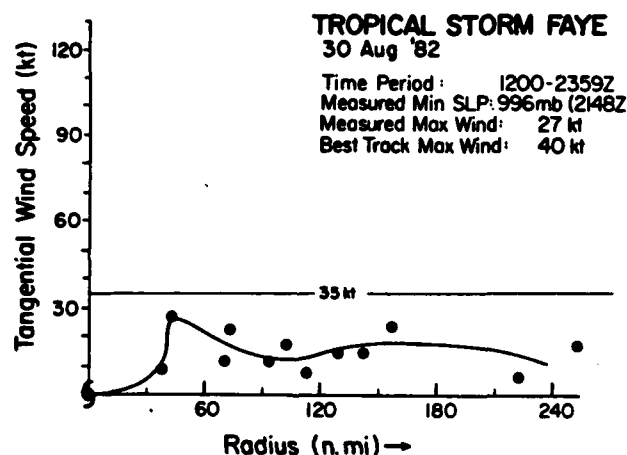

TROPICAL STORM FAYE
30 Aug '82

Time Period: 1200-2359Z
Measured Min SLP: 996 mb (2148Z)
Measured Max Wind: 27 kt
Best Track Max Wind: 40 kt

Fig. 2.8. Dissipating Tropical Storm Faye's wind profile dropped below 35 kt so that R-30 could not be sensed.

TYPHOON LEX
1 Aug '82

Measured Min SLP: 963 mb
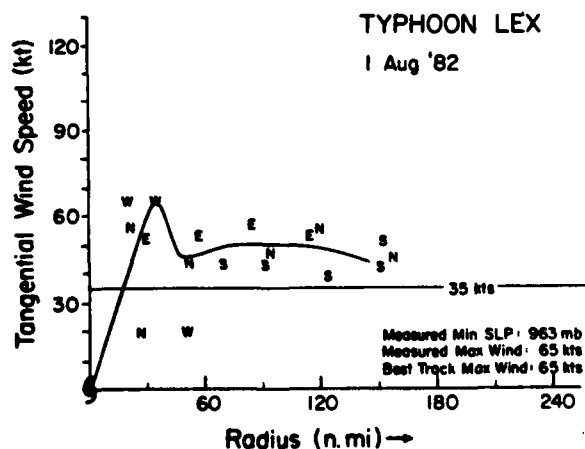Measured Max Wind: 65 kts
Best Track Max Wind: 65 kts

Fig. 2.9. Typhoon Lex's size of 30 kt surface winds (35 kt at 700 mb) was not measured during this mission.

3) where R-30 lay inside 250 n mi but was not sensed (Fig. 2.9).

b) <u>R-50</u> - the average radius to which the 50-kt surface wind speeds extended from the cyclone center.

The areal extent of 50-kt surface wind speeds (59 kt at 700 mb) was used to determine the radial extent of the beginning of damaging wind speeds and was also a requirement for the JTWC warnings. This radius was almost always found inside 150 n mi and was thus, most often, a four quadrant average.

2.7 Various Intensity Parameters

The label for the curves shown in this report that depicts a wind profile includes three reference points for cyclone intensity: measured minimum sea-level pressure, flight level measured maximum winds, and 'Best Track' maximum winds. The intent was to provide a common point of reference for readers who relate to different intensity measurements. The measured SLP_{min} was the most reliable measure of intensity and was included to show consistent changes occurring at the core of the cyclone. The maximum wind speed was far more difficult to estimate, yet was vital to the forecasting problem. Two maximum winds were listed: the maximum wind measured in flight in the MOT coordinate system (relative to the cyclone's motion), and the 'Best Track' maximum wind analyzed in a natural coordinate system (cyclone motion not considered). The 'Best Track' maximum wind was often determined by applying the minimum sea-level pressure/maximum wind relationship which Atkinson and Holliday (1977) derived.

$$V_{max} = 6.7 \ (1010 - SLP_{min})^{.644},$$

V_{max} is the maximum surface wind. They compared minimum sea-level pressure to the peak gusts observed at coastal land stations during

eyewall passage and reduced the speed to a one-minute average. Therefore, these three measures (minimum sea level pressure, maximum observed speed and 'Best Track' wind speed) will differ for each cyclone but are to be referred to in order to gauge the cyclone's intensity. For the pu pose of this study SLP_{min} was used exclusively as the intensity parameter.

The next chapter discusses the general statistics of this flight information.

3. GENERAL STATISTICS ON THE VARIABILITY OF INTENSITY, STRENGTH, R-30 AND R-50

In order to better understand the tropical cyclone wind profile and its variations, it is helpful first to perform a statistical analysis of each portion of the radial profile in order to answer the following questions. How are cyclone intensity, strength and size (R-30 and R-50) related to each other? How are these structural characteristics related to latitude, season, time of day and cyclone motion? Finally, how rapidly can a tropical cyclone intensify, change its strength or expand its radius of 50-kt winds?

3.1 Intensity, Strength, R-30 and R-50

One of the advantages of this data set of over 500 flight missions was that a full range of cyclone intensities, strengths, and sizes were sampled in the northwestern Pacific from 1980-1982. No attempts were made to sample one intensity class over another, so the data provided a reliable basis for infering averages and extremes. As Fig. 3.1 shows, the average intensity of all cases treated was 971 mb (68 kt). This figure plots central pressure against the measured 700 mb maximum wind showing a correlation of .88. However, since there was a higher degree of reliability in the central pressure measure, this paper will follow the convention established by Atkinson and Holliday (1977) of using measured minimum sea level pressure as a measure of cyclone intensity, categorized as follows:

TROPICAL DEPRESSION   > 997 mb
TROPICAL STORM   997 - 977 mb
TYPHOON   976 mb - 909 mb
SUPERTYPHOON   ≤ 910 mb

Strength (Fig. 3.2) ranged from 3 kt to 70 kt, averaging 37 kt overall.

The distribution of R-30 and R-50 averaged 102 n mi (Fig. 3.3) and 62 n
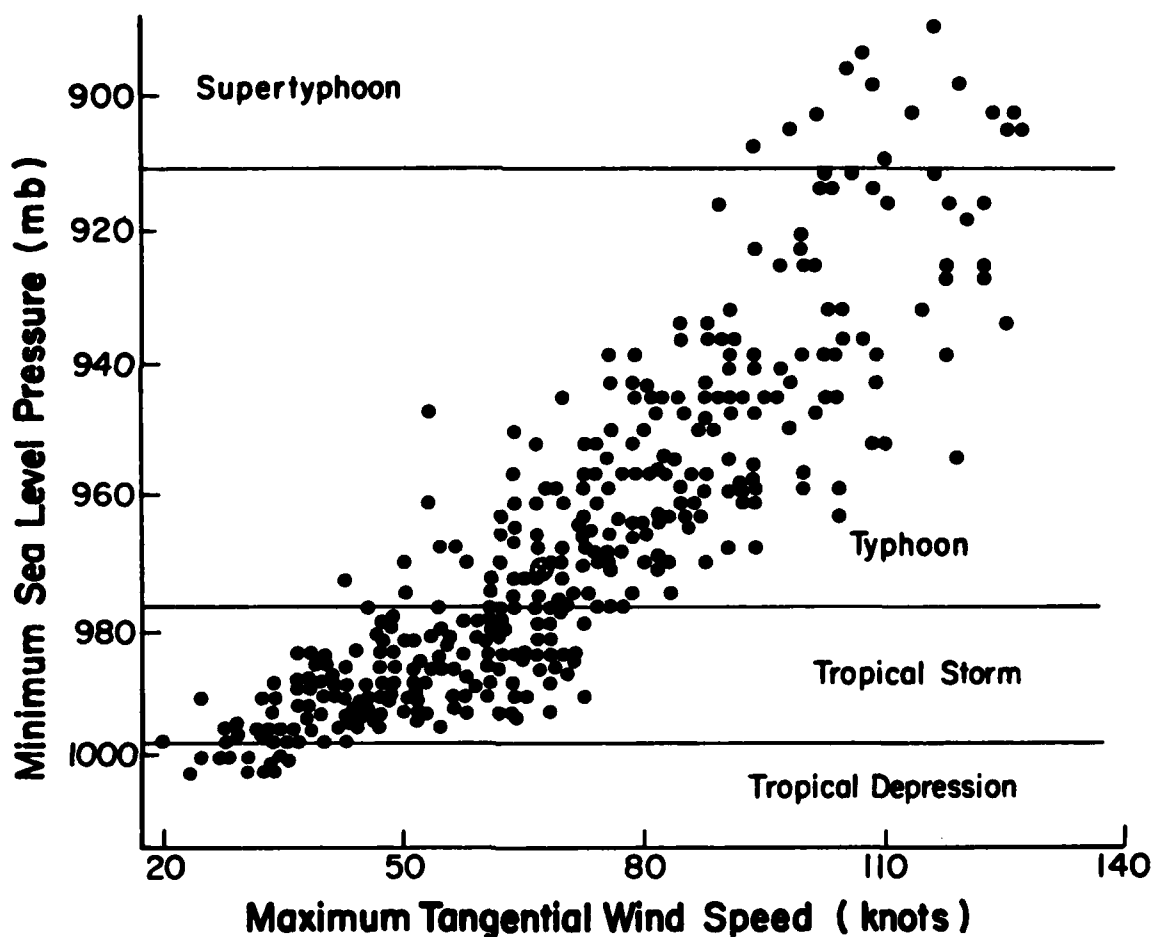
mi (Fig. 3.4), respectively.

Fig. 3.1.   Intensity vs. measured maximum tangential wind speed (MOT
            SYSTEM - relative to the cyclone center). The mean value,
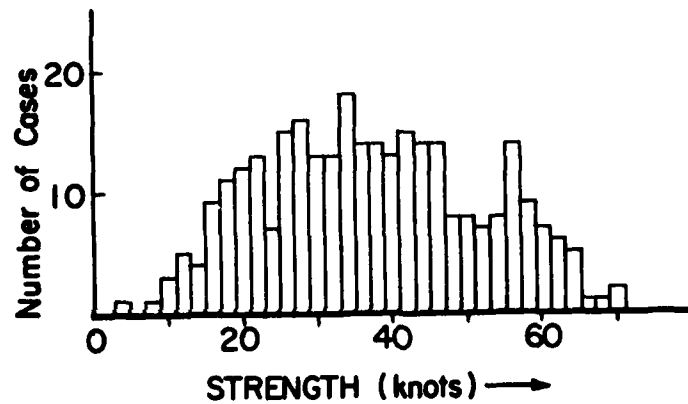   given by the circled x is 971 mb (68 kt).

Fig. 3.2. Histogram of strength for the 1980-82 period (12-hour intervals.
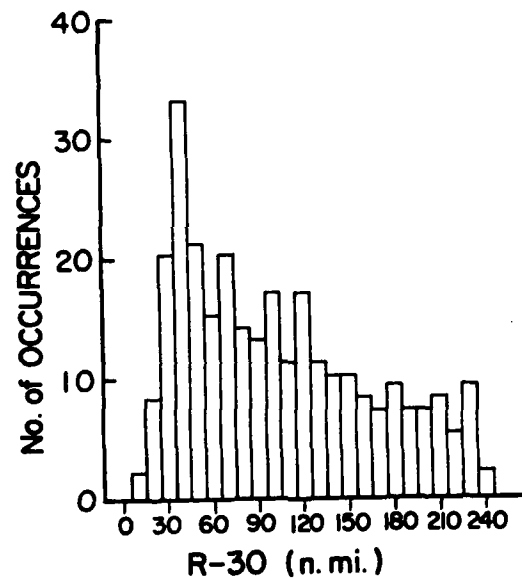

Fig. 3.3. Histogram of R-30 for each 12-hr interval (extent of 30-kt surface winds in n mi and not measured beyond 250 n mi).
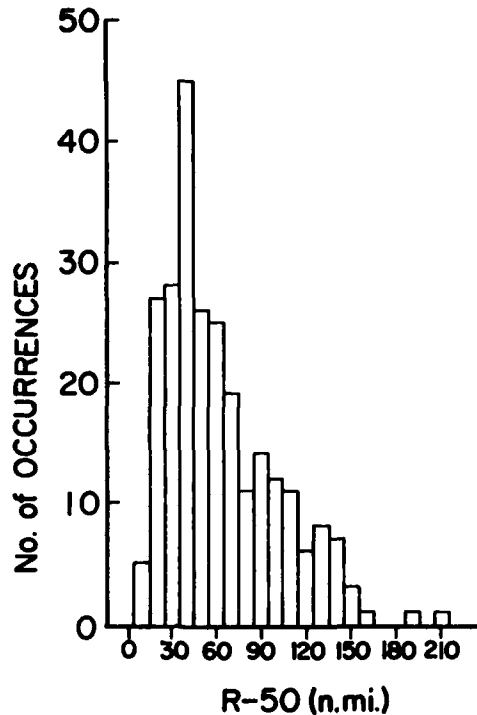
Fig. 3.4. Histogram of R-50 for each 12-hr interval (extent of 50-kt winds in n mi).

3.2 Latitude

This data sample included tropical cyclones from genesis to the extratropical transition, with the latitude of the cyclone center ranging from 6° to 40°N. The average latitude of the over 500 flight missions during 1980 to 1982 was 18°N, $\pm\ 6^\circ$ standard deviation as seen in Fig. 3.5. The greatest frequency of flight-measured center positions fell between 12° to 22°N. Figure 3.6 depicts cyclone intensity by latitude. The most intense systems occurred near 15° to 20°N. Cyclone strength (Fig. 3.7), by contrast, appeared to increase with latitude. This is likely a result of the cyclones' interaction with larger scale wind fields to the north. One might have expected that the latitude of maximum intensity would match the latitude of maximum strength. This was not the case however.
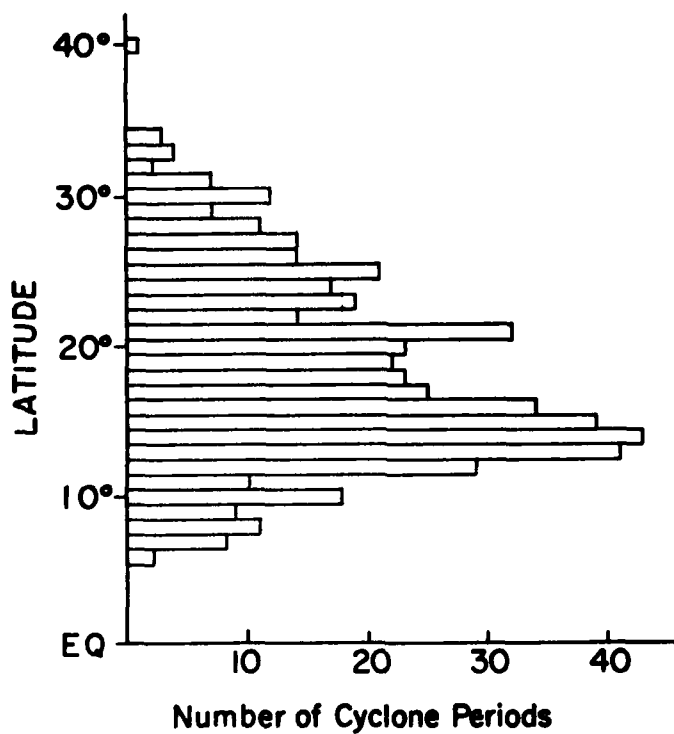
Fig. 3.5. Latitudinal distribution of the mean cyclone center position
for the 517 flight misions. Average latitude = 18°N, $\pm 6^{O}$
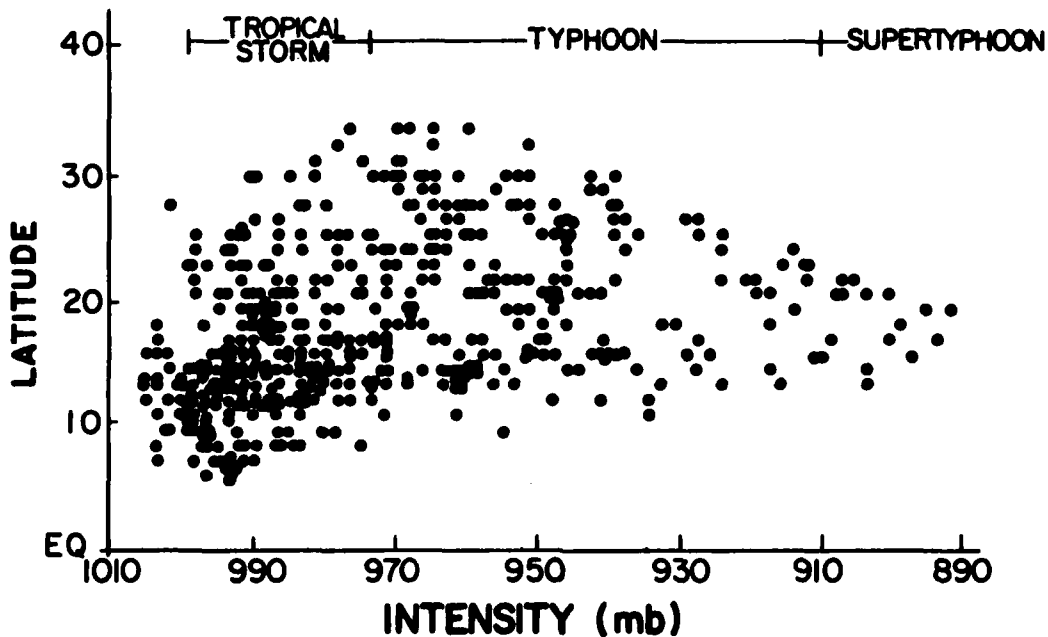standard deviation.

Fig. 3.6. Intensity distribution by latitude indicates: 1) only very
weak systems are found below 10°; 2) the entire range of
intensities can occur between 10° and 20°; and 3) there
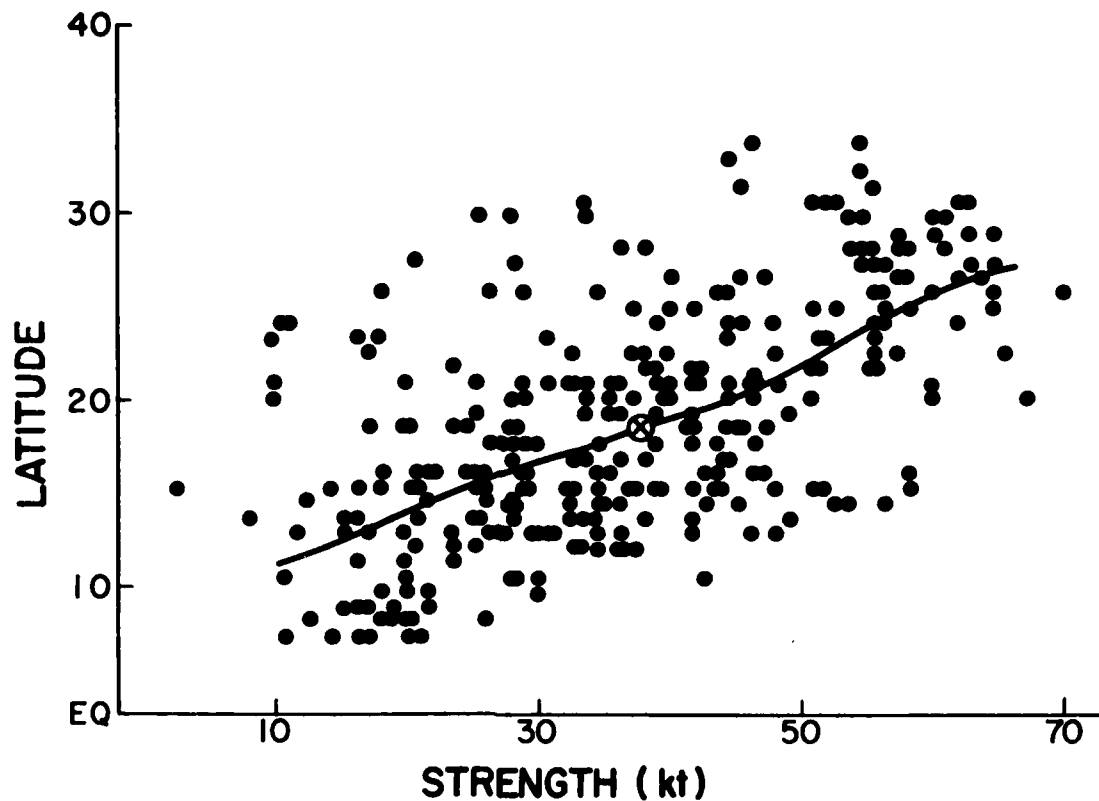appears to be an upper limit to the intensity above 20°.

Fig. 3.7. Strength vs. latitude. Centroid (cross) shows average pt.
Line runs through the median latitude by strength.

It appeared that the central core responded to different stimuli than

the strength region. Figures 3.8 and 3.9 show that, in the mean, R-30

and R-50 also increase with latitude.

3.3 Stratification by Month

During 1980 to 1982, tropical cyclones occurred from March through

December. Figure 3.10 portrays cyclone intensity by month, with

September and October the months of most intense systems. Figure 3.11

shows that the greatest strength values were also found in September and

October but with less of a difference from month to month throughout the

summer period. Figures 3.12 and 3.13 reveal roughly similar peaks in

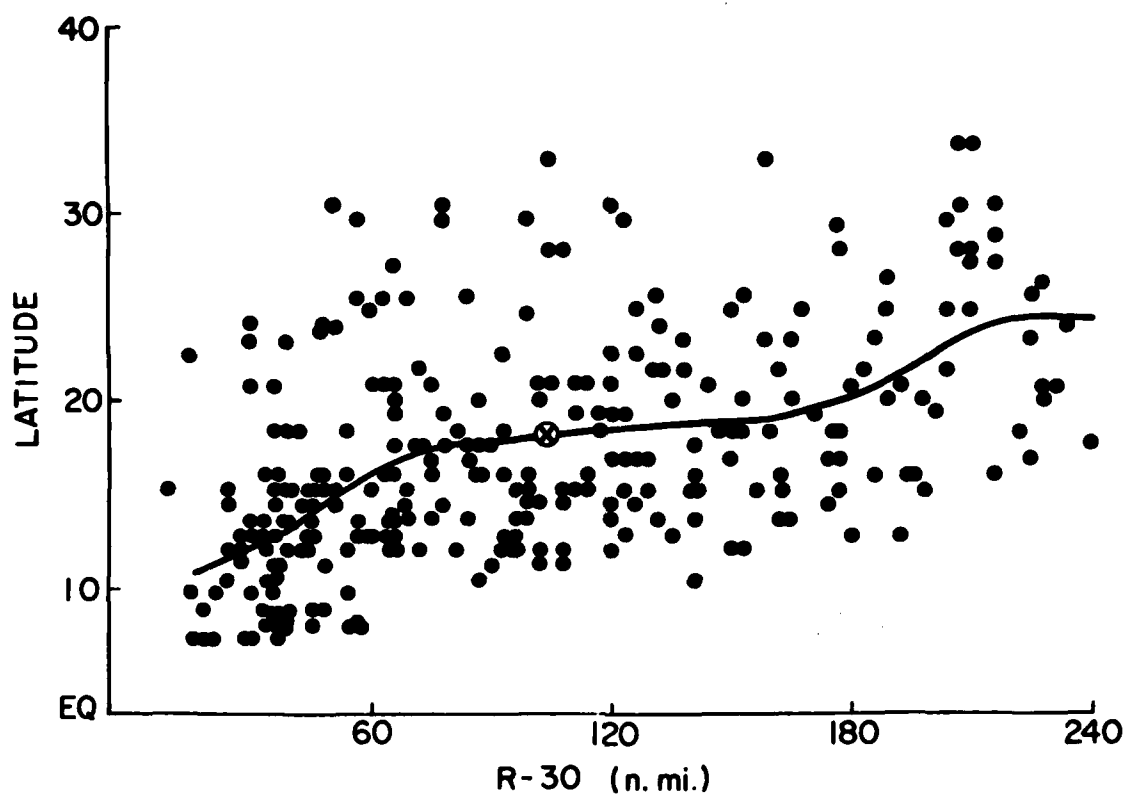R-30 and R-50 except for the unusually large Typhoon Thad in August.

Fig. 3.8. Latitude vs. extent of 30-kt surface winds. The curve runs through the median latitude by radius.
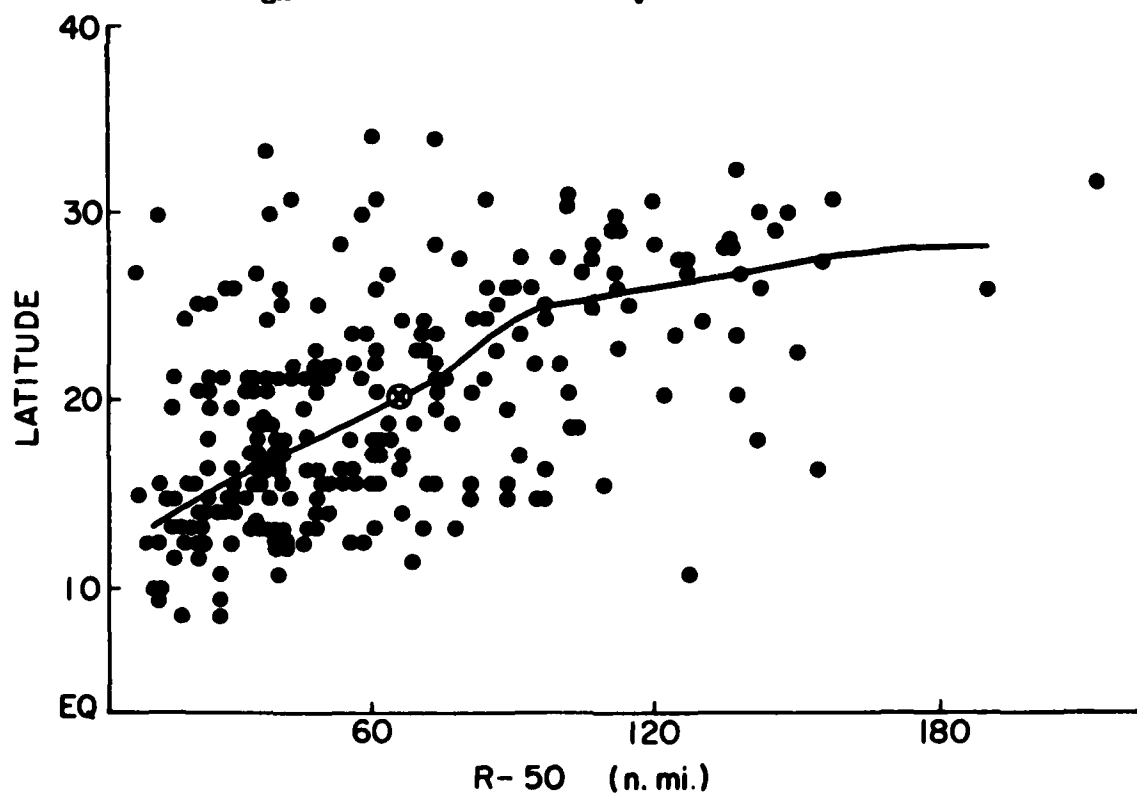

Fig. 3.9. Radial extent of 50-kt surface winds vs latitude. The curve runs through the median latitude by radius.
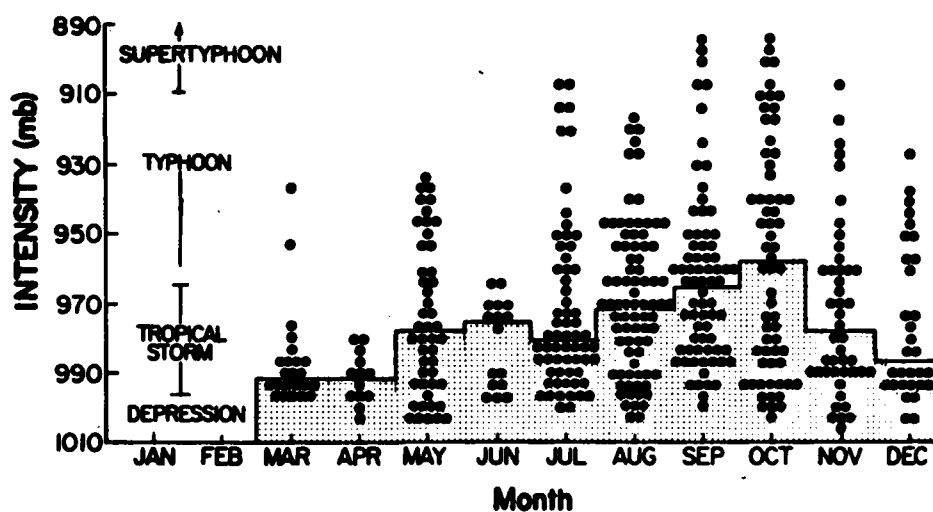
Fig. 3.10.   Intensity distribution by month. Stippled area indicates
the region from the lowest to the median intensities for
each month.
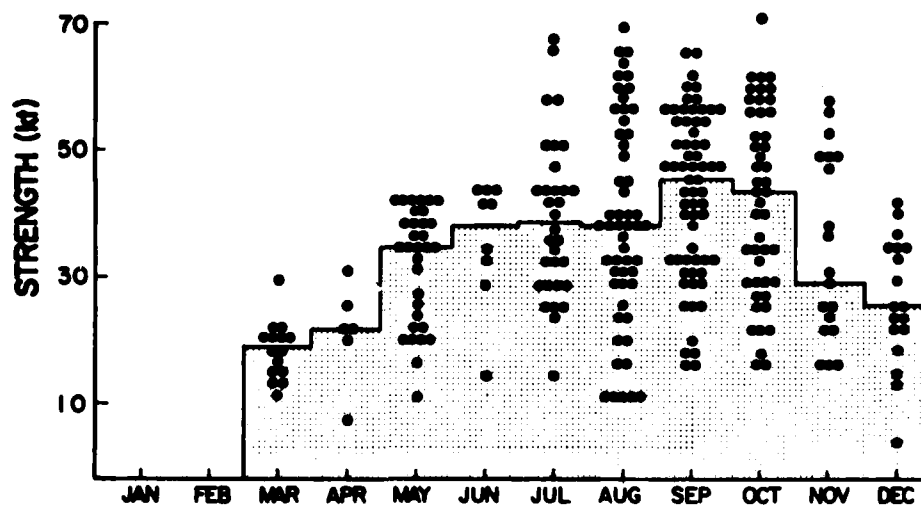
Fig. 3.11.   Distribution of strength by month. Stippled area indicates
the region from the lowest to the median strength values.

Fig. 3.12. Monthly distribution of the radius of 30-kt winds (MOT) for
the 1980-82 period. Stippled area indicates the region of
the smallest half of the cyclones for each month.

Fig. 3.13. Monthly distribution of R-50 (extent of 50-kt surface winds
in nautical miles). The stippled area indicates the region
of the smallest half of the cyclones by month.

3.4 Diurnal Differences

Flight missions were roughly distributed by daylight and nighttime hours, affording a convenient way to detect diurnal differences. Average wind profiles shown in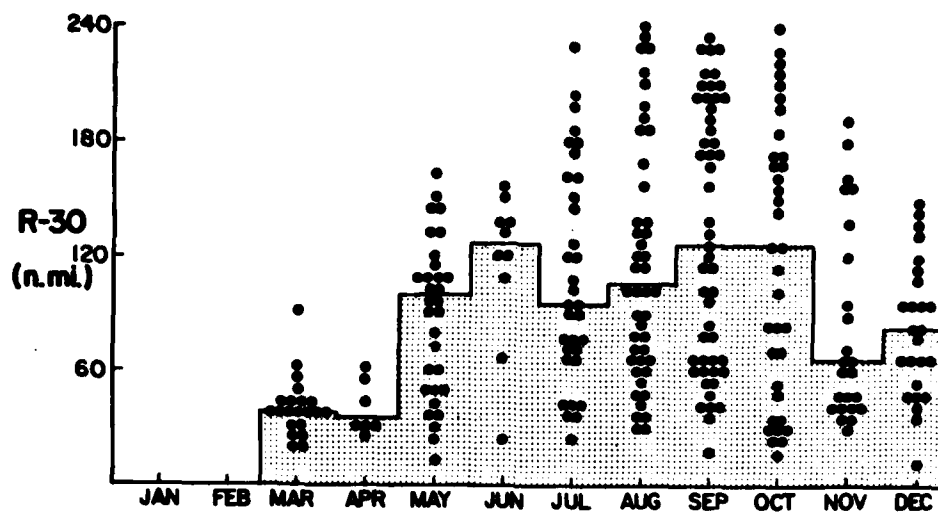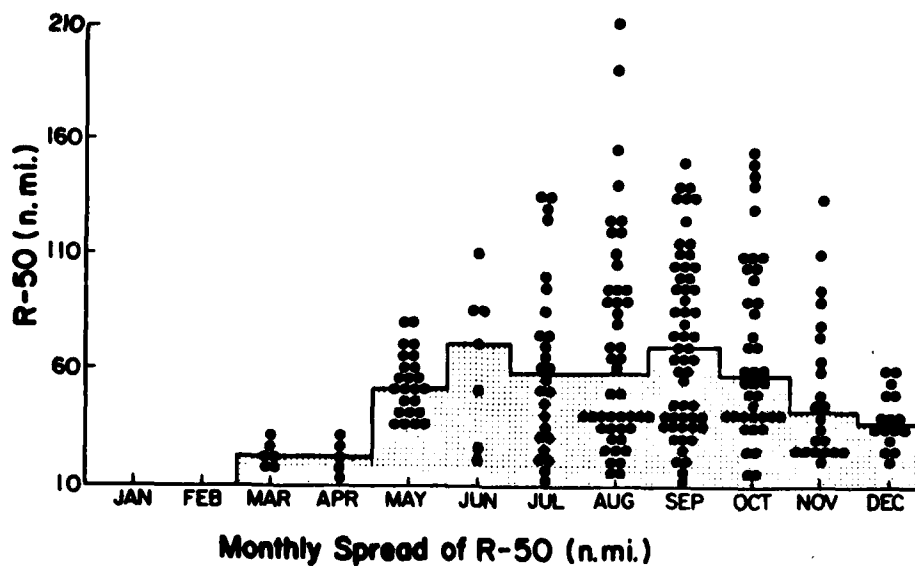 Fig. 3.14 were divided into four intensity classes. Each intensity class showed no significant difference from day to night along any portion of the radial profile. In the northwestern Pacific, 00 to 12Z corresponds roughly to 9 to 21 Local Time (LT); similarly, 12 to 24Z corresponds to 21 to 09 LT (night). No significant differences were found in cyclone intensity, strength, or size. Nor was there a preference for changes in intensity or strength to occur more rapidly from day to night or night to day.

3.5 Cyclone Motion Effects

Cyclone track headings of 1980-82 as shown in Fig. 3.15 (a and b) were similar to the long period climatological view (Gray, 1981). Although 280° was most frequently the heading (the mode), the mean direction was 320° indicating that the cyclones headed west for a significant part of their life cycles before recurving. This was also evident in Fig. 3.16 which depicted cyclone direction of motion by intensity, showing that the bulk of the tropical storms (34 to 63 kt) headed toward the west-northwest. Note that all the supertyphoons in this sample followed a pattern of track heading from west to northwest. However, for cyclones of largest strength (Fig. 3.17) and largest radius of 30 kt wind (Fig. 3.18) motion can be anywhere from west to northeast thereby retaining their large strength values beyond recurvature.

Cyclone speed of motion appeared to bear little relation to the intensity, strength, R-30, or intensity change of the tropical cyclone.
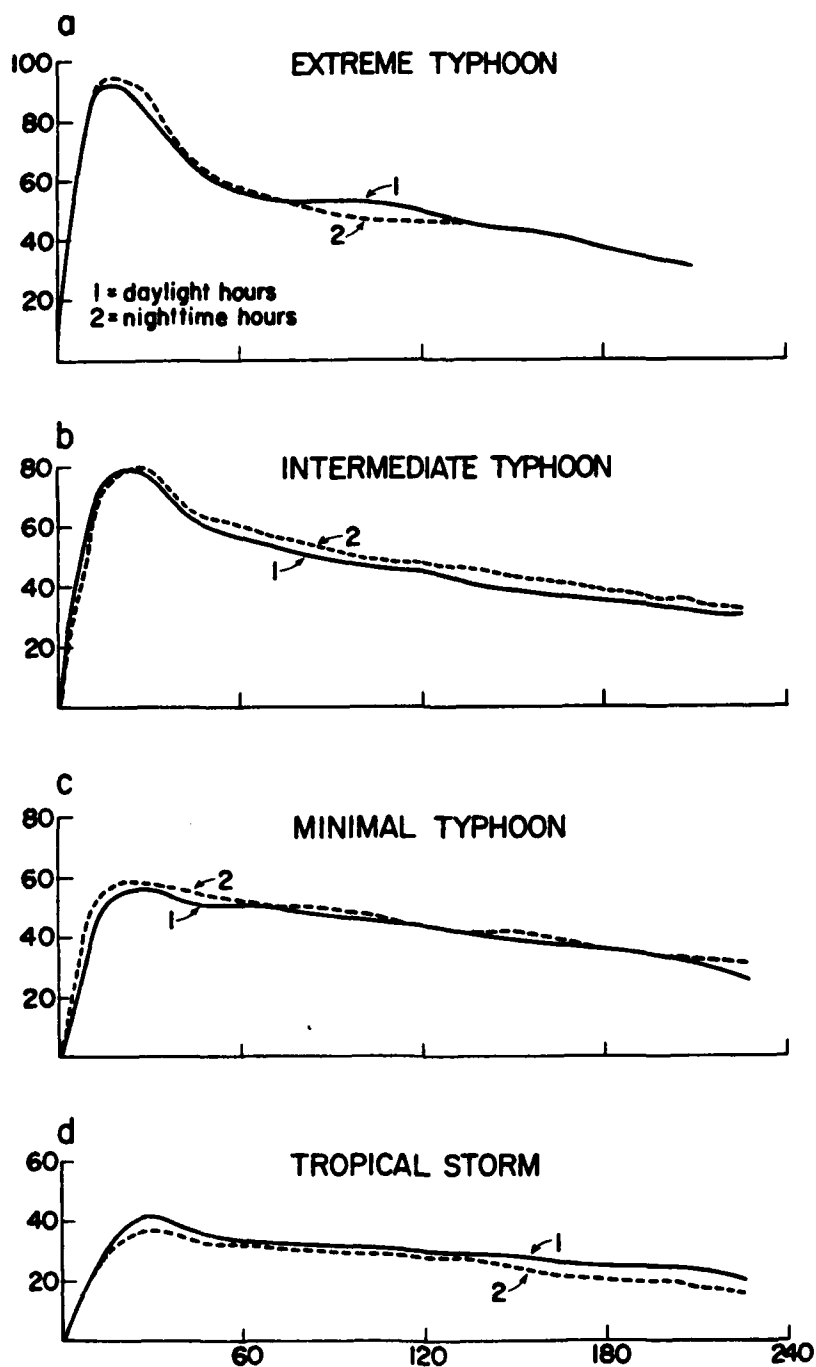
Fig. 3.14. The diurnal profiles by intensity class. Solid curves
represent data gathered between 00 to 12Z, dashed curves
between 12 to 24Z (nighttime hours 21 to 09 LT). Intensity
classes are as follows: extreme typhoon, below 920 mb;
intermediate typhoon, 920-950 mb; minimal typhoon, 950-976
mb; tropical storm, 977-999 mb.
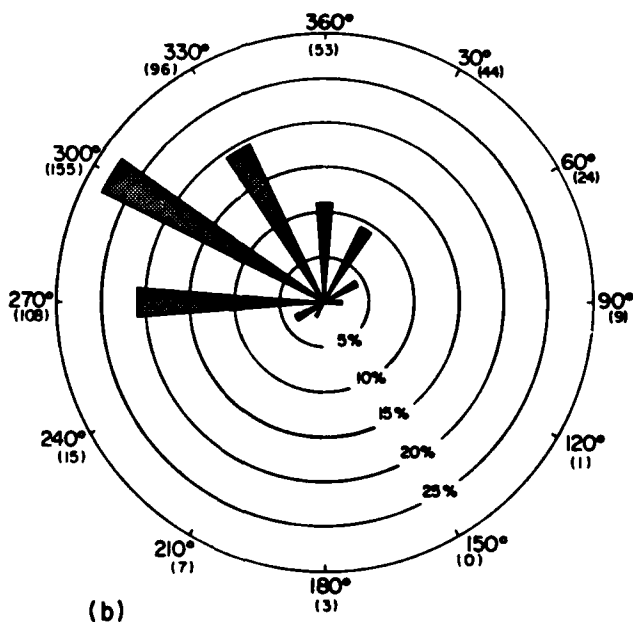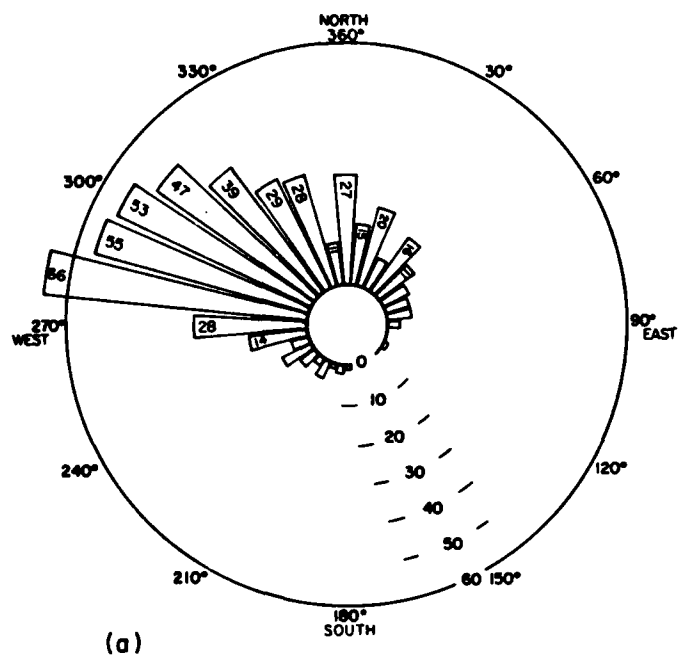
Fig. 3.15. Frequency distribution showing cyclone direction of motion
for the 517 missions. a) number of cases at each 10°
interval, b) percent of total at each 30° interval. Number
of cases for each 30° interval is in parentheses.
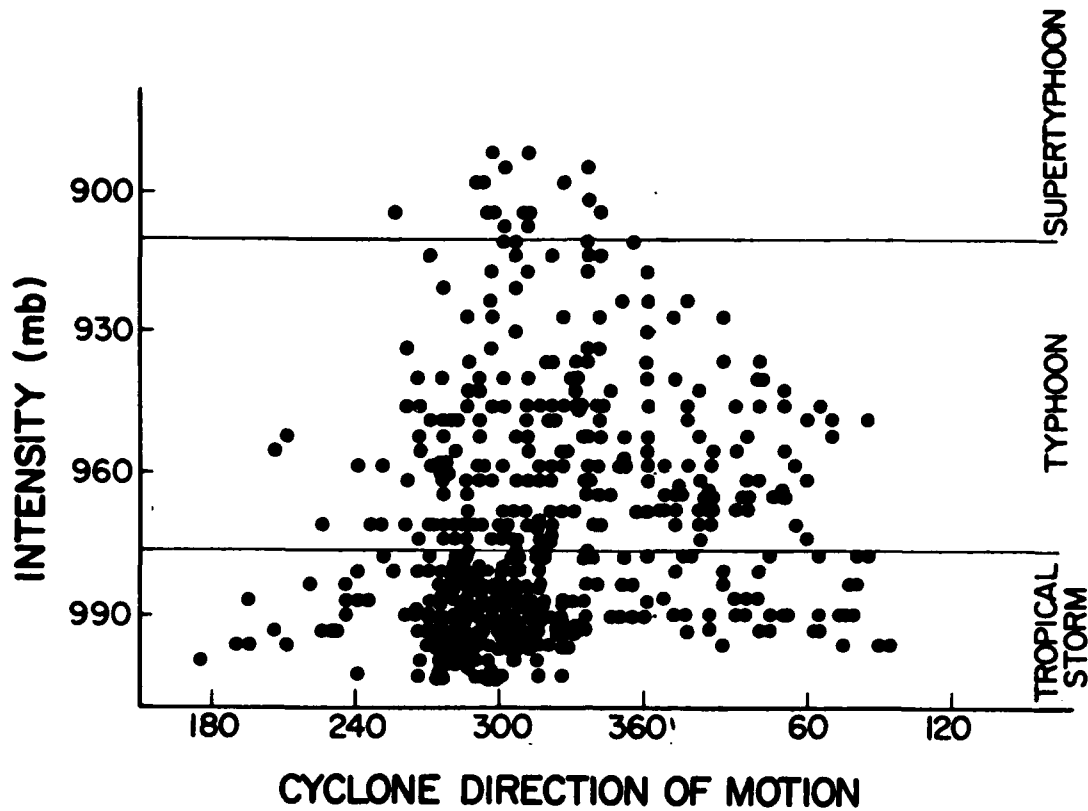
Fig. 3.16. Intensity broken down by the cyclone centers direction of motion (in °).
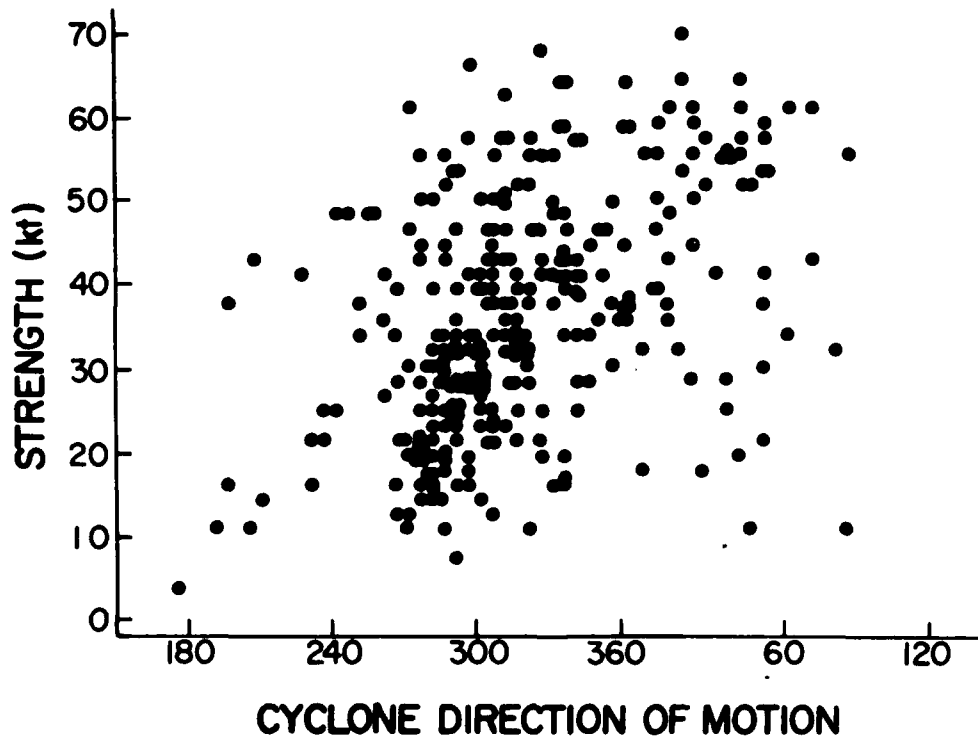
Fig. 3.17. The cyclone's strength (kt) remains unaffected by the cyclone center direction of motion (in °).

31
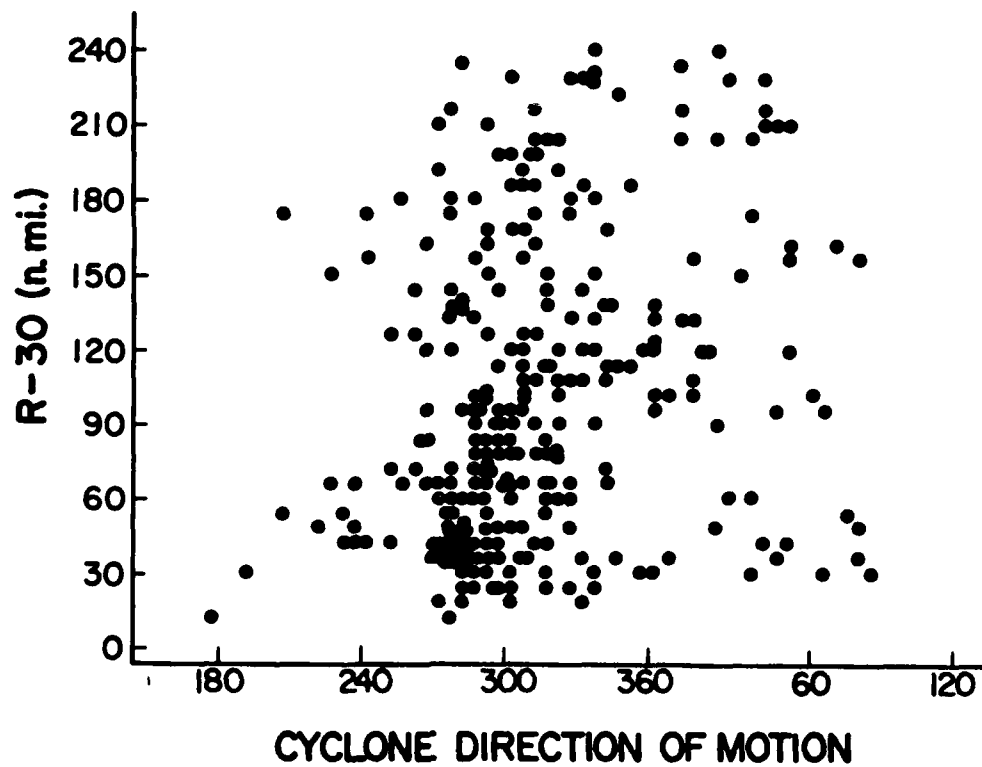
Fig. 3.18. The size (R-30 in n mi) of the cyclone is relatively unaffected by the direction in which the cyclone center is moving.
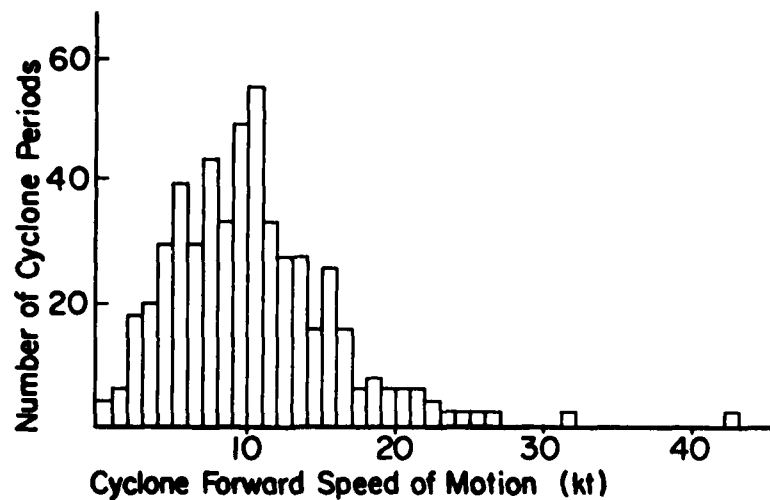
Fig. 3.19. Histogram of cyclone forward speed of motion per flight mission. Average is 11 kt.
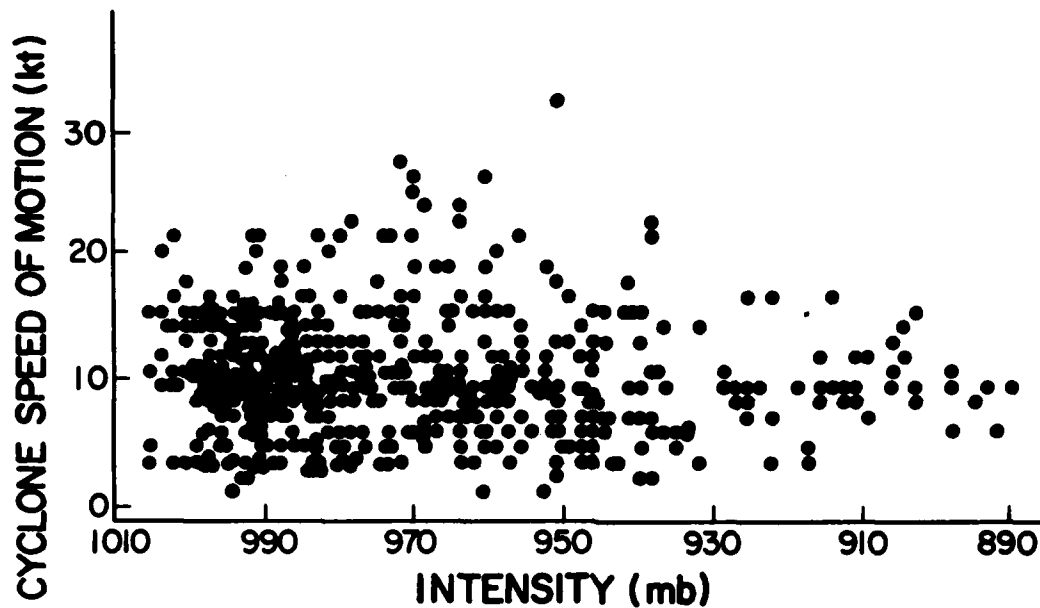
Fig. 3.20. Intensity vs. cyclone speed of motion (correlates at .13).

The range of speeds shown in Fig. 3.19, extended to 43 kt and averaged 11 kt. This average forward speed of motion of 11 kt applied to cyclones of all classes (Fig. 3.20), all strengths from 3 kt to 70 kt (Fig. 3.21), and all sizes whether by R-30 (Fig. 3.22) or R-50 (Fig. 3.23). However, there was a noticeable relationship between the 12-hour change of intensity and cyclone speed. As Fig. 3.24 indicates, the most rapid deepeners clustered near the mean forward speed of 11 kt. Similarly, the cyclones moving most rapidly (more than twice the average speed of motion) exhibited the least change in intensity.

3.6 Temporal Changes Along the Wind Profile

As each flight mission performed the same flight pattern every 12 hours, it was possible to make 12-hour measurements of the changes of cyclone intensity, strength, and R-50. These are referred to as half-day increment changes. Figure 3.25 provides a conceptualized view of the changes in cyclone intensity, strength, and size which can occur.
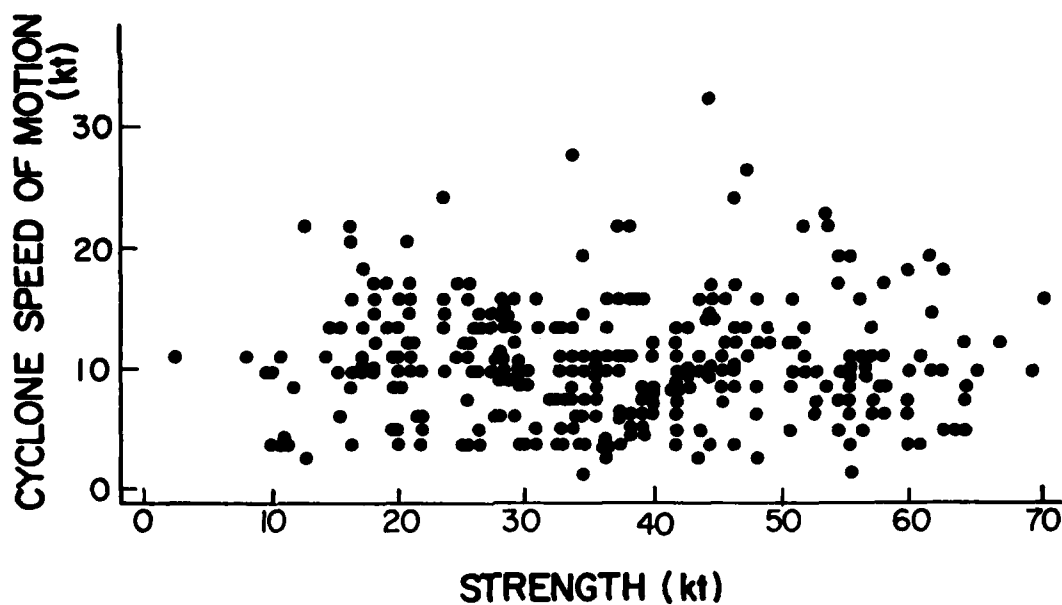
Fig. 3.21. Strength (kt) vs. cyclone speed of motion (kt) shows little indication that cyclone speed of motion is associated with cyclone strength.
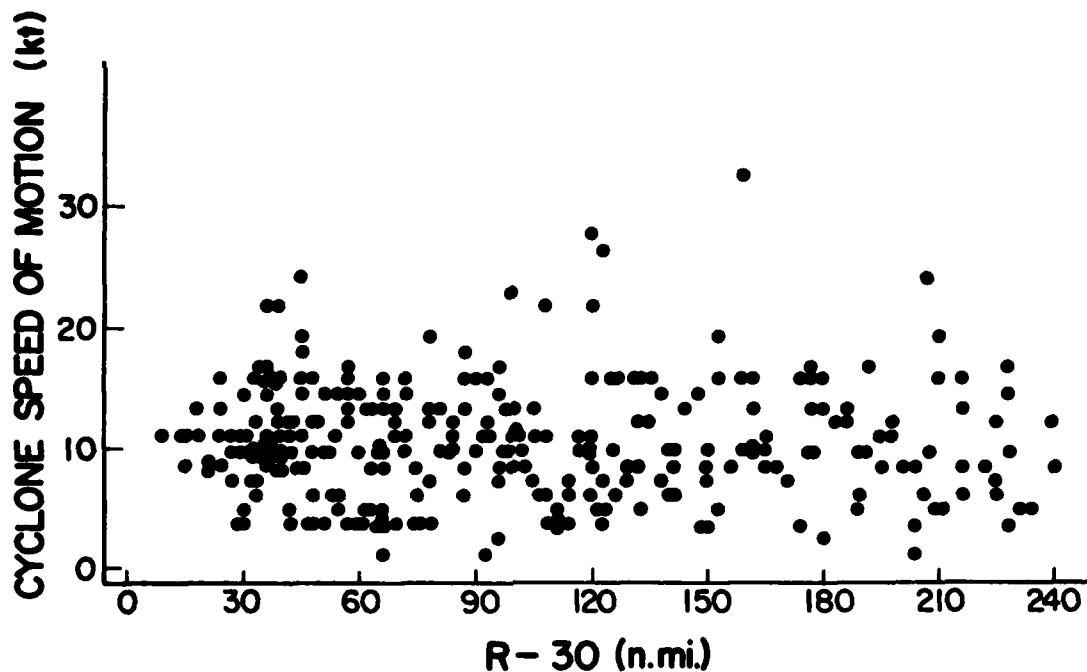
Fig. 3.22. R-30 (extent of 30-kt surface winds) vs. cyclone speed of motion.
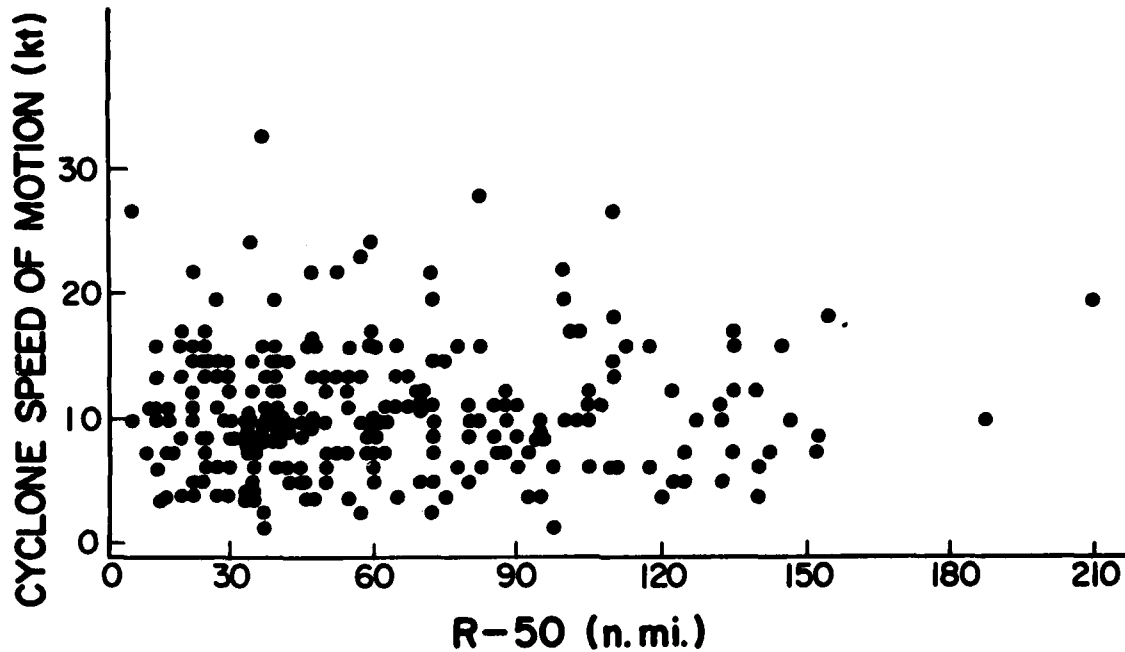
Fig. 3.23. R-50 (extent of 50 kt surface winds) vs. cyclone speed of motion.
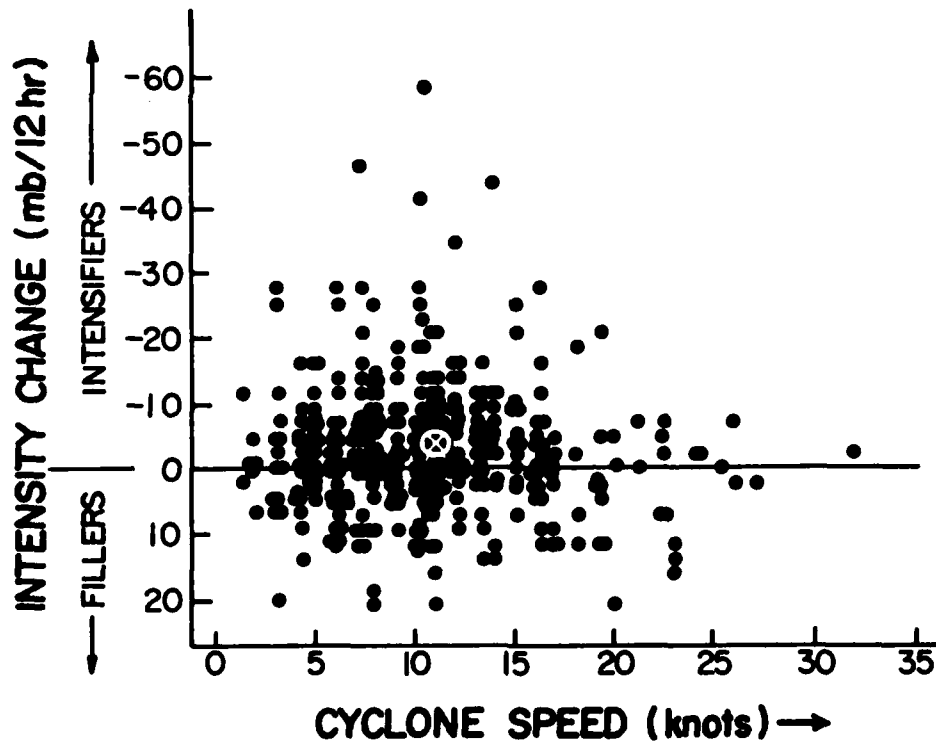
Fig. 3.24. Intensity change which occured over a 12-hour period (mb per 12 hours) indicates that fillers show no preference with respect to cyclone speed but that cyclones intensify less rapidly when the cyclone speed is large. Centroid indicated by ⊗.
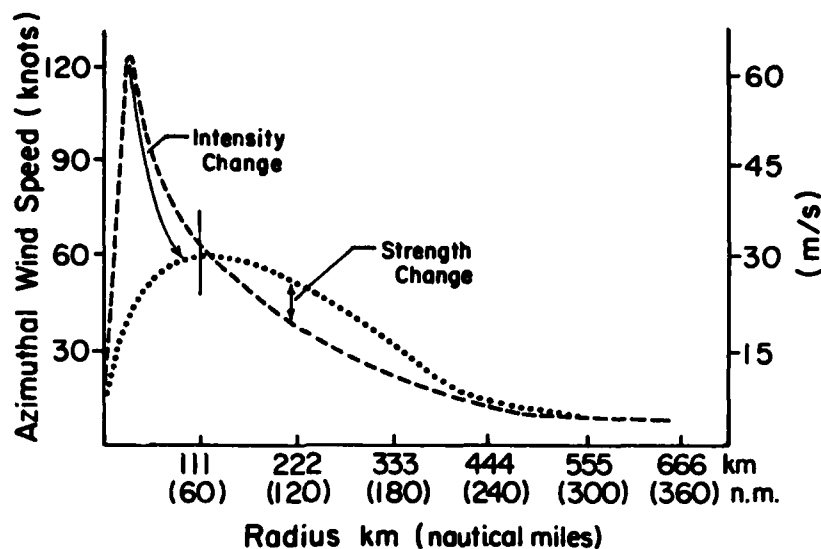
Fig. 3.25. Conceptual view of changes in the wind profile.

Of the 66 cyclones treated here, the average change in intensity was 7 mb per 12 hours (Fig. 3.26) whether the cyclone was filling or intensifying. It appeared that the maximum filling rates were 20 mb/12 hours, while maximum deepening rates approached 60 mb/12 hours. The most rapid deepener was Supertyphoon Wynne with a drop of 59 mb in 12 hours (79 mb in 20 hours). Wynne accomplished this intensity change while showing no change in strength.

Strength changes averaged 5 kt in 12 hours as seen in Fig. 3.27. Figure 3.28 depicts the most dramatic change in strength when Supertyphoon Kim gained 15 knots of wind strength while its central intensity rapidly increased.

Size changes could be equally dramatic. Figure 3.29 shows a growth in the 50 kt wind radius of 102 n mi/12 hours for the case of Typhoon Owen at the same time that the center was filling from 939 mb to 950 mb. R-50 changes occurred most frequently between $\pm$ 22 n mi per 12 hours as
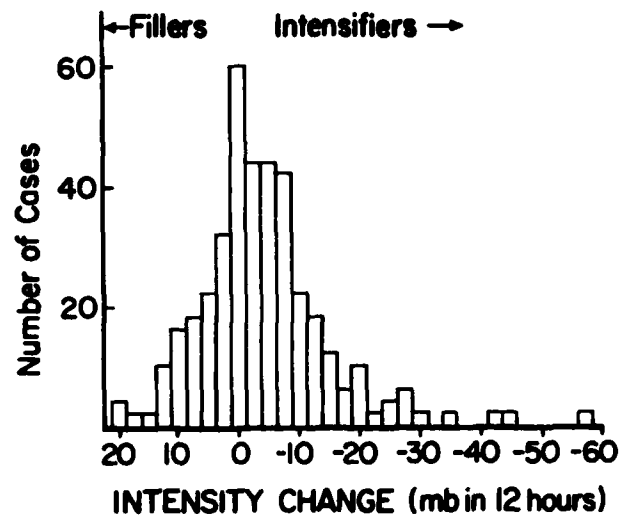
Fig. 3.26. Histogram of intensity changes over a 12-hour period for the 1980-82 period.
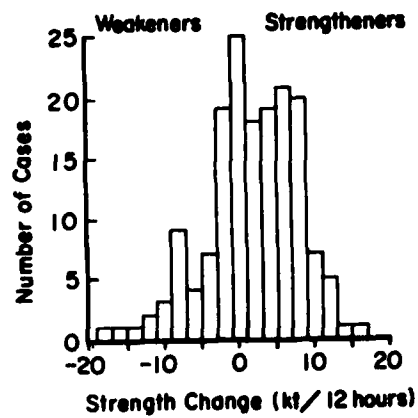
Fig. 3.27. Distribution of strength changes which occurred over a 12-hour period.
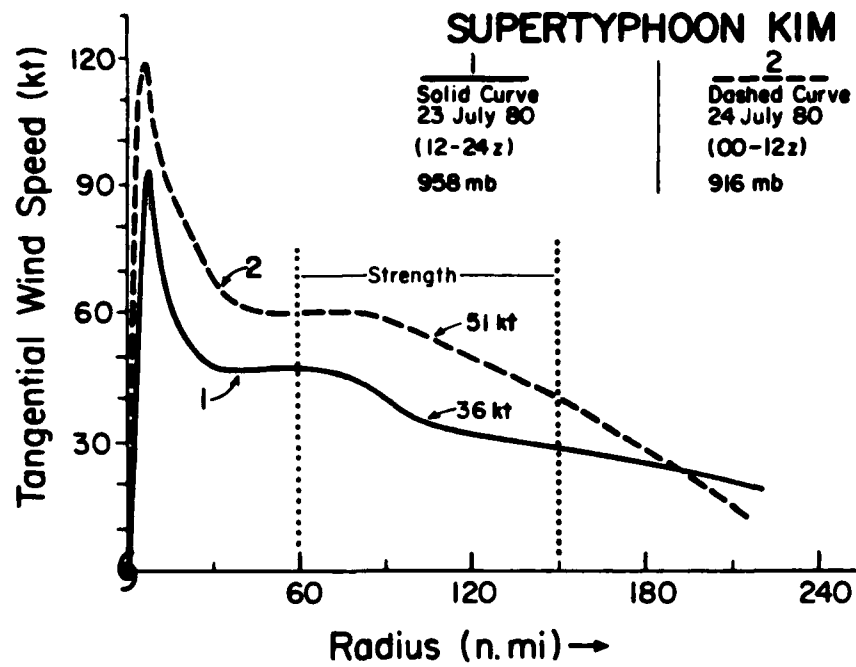
Fig. 3.28. Supertyphoon Kim strengthened 15 kt in a 12-hour period.
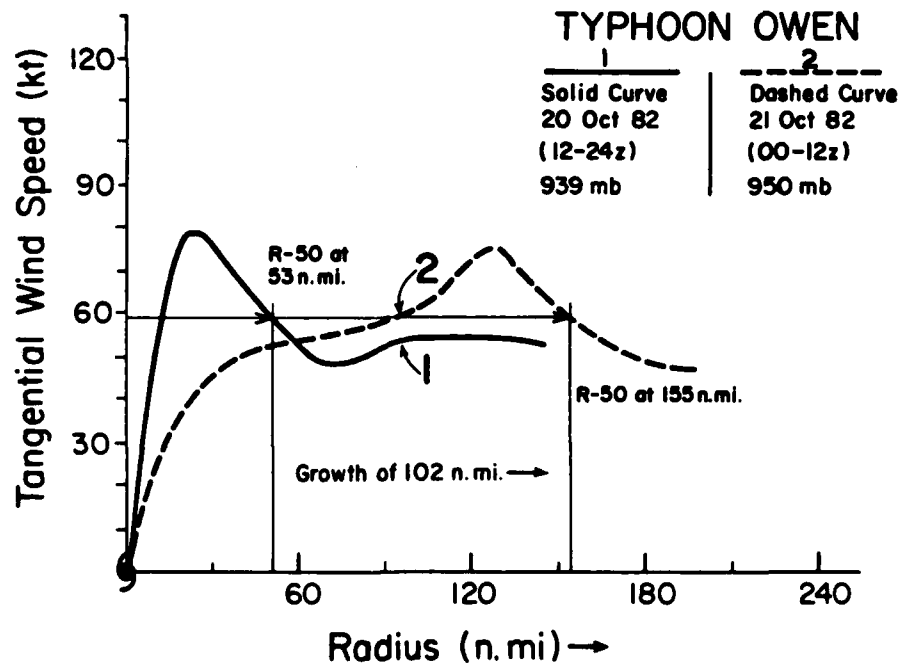
Fig. 3.29. Typhoon Owen changes R-50 rapidly in 12 hours as the radius of maximum wind moves out.

shown in Fig. 3.30. Statistics on the changes in R-30 were not
considered to be very representative due to the number of cyclones whose
30-kt wind extended beyond 250 n mi (limit of the flight mission), thus
biasing the data sample toward smaller cyclones. Figure 3.31 portrays
the rapidity with which all of the wind structural features could
decrease when environmental weakening influences were especially strong.
Over a 24-hour period, Typhoon Kit filled by 22 mb, lowered its strength
by 12 kt and contracted in R-30 by 50 n mi as a mid-latitude trough
approached from the northwest in December.

These statistics provide a depiction not only of how intense,
strong and large a tropical cyclone could become, but also how quickly
these changes occurred. The effects of latitude, month, time of day and
cyclone motion appeared to be subtle on the cyclone's intensity,
strength and size. Yet, intensity, strength, and size of a cyclone can
interact with each other. Therefore, we turn our attention next to the
relationships between intensity, strength, R-30 and R-50.
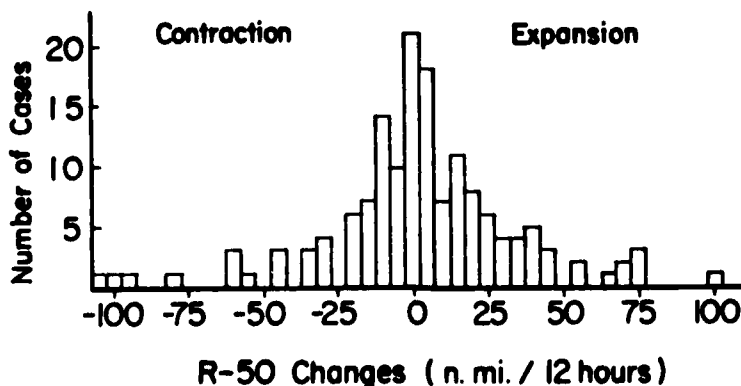
Fig. 3.30. Histogram of the change in the size of 50 kt winds (R-50)
            over a 12-hr period.
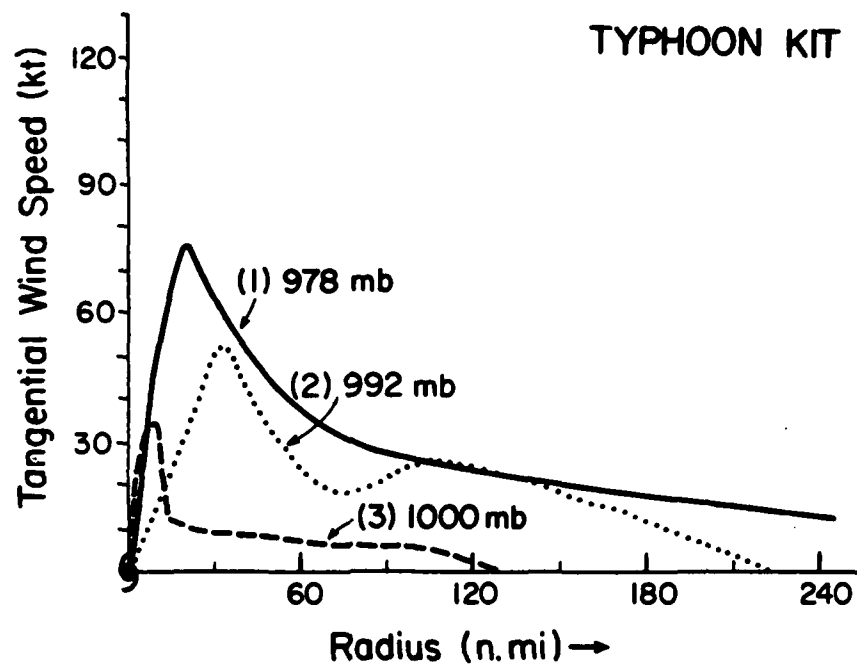
Fig. 3.31. Typhoon Kit (1981) rapidly weakened as a mid-latitude trough approaches from the NW. (1 - (solid curved) 19 Dec 0000-1200Z; 2 - (dotted curve) 19 Dec 1200-2400Z; 3 - (dashed curve) 20 Dec 000-1200Z)

4. RELATIONSHIPS BETWEEN CHANGES OF INTENSITY AND STRENGTH, R-30 AND R-50

Understanding the interaction of one portion of the wind profile with the others is vital to forecasters and researchers alike. For instance, given the central pressure of a cyclone, can we predict the accompanying strength and extent of gale force winds? Similarly, if the central pressure drops, does the strength increase accordingly? Does the entire wind profile build up or do only sections of it increase at a time?

4.1 Intensity vs. Strength and Size

In comparing a cyclone's intensity with its strength, Fig. 4.1 illustrates a great amount of variability. Although the least amount of scatter existed in the tropical storm stage, suggesting some forecasting skill, once a cyclone attained typhoon intensity or forms an eye, the ability to relate cyclone intensity and strength was nearly lost. For example, typhoons with central pressures of near 960 mb exhibited strengths ranging anywhere from 20 kt to 60 kt (a three-fold difference). The most intense cyclone was Supertyphoon Wynne (central pressure of 890 mb) with an average strength of only 35 kt. By contrast, Typhoon Vernon had a central pressure of 940 mb but had a much greater strength of 70 kt. This large variability among intensity and strength makes for a very difficult forecasting problem.

Each cyclone followed a distinctly different pattern of intensity and strength changes. Figure 4.2 depicts four examples. Typhoon Betty
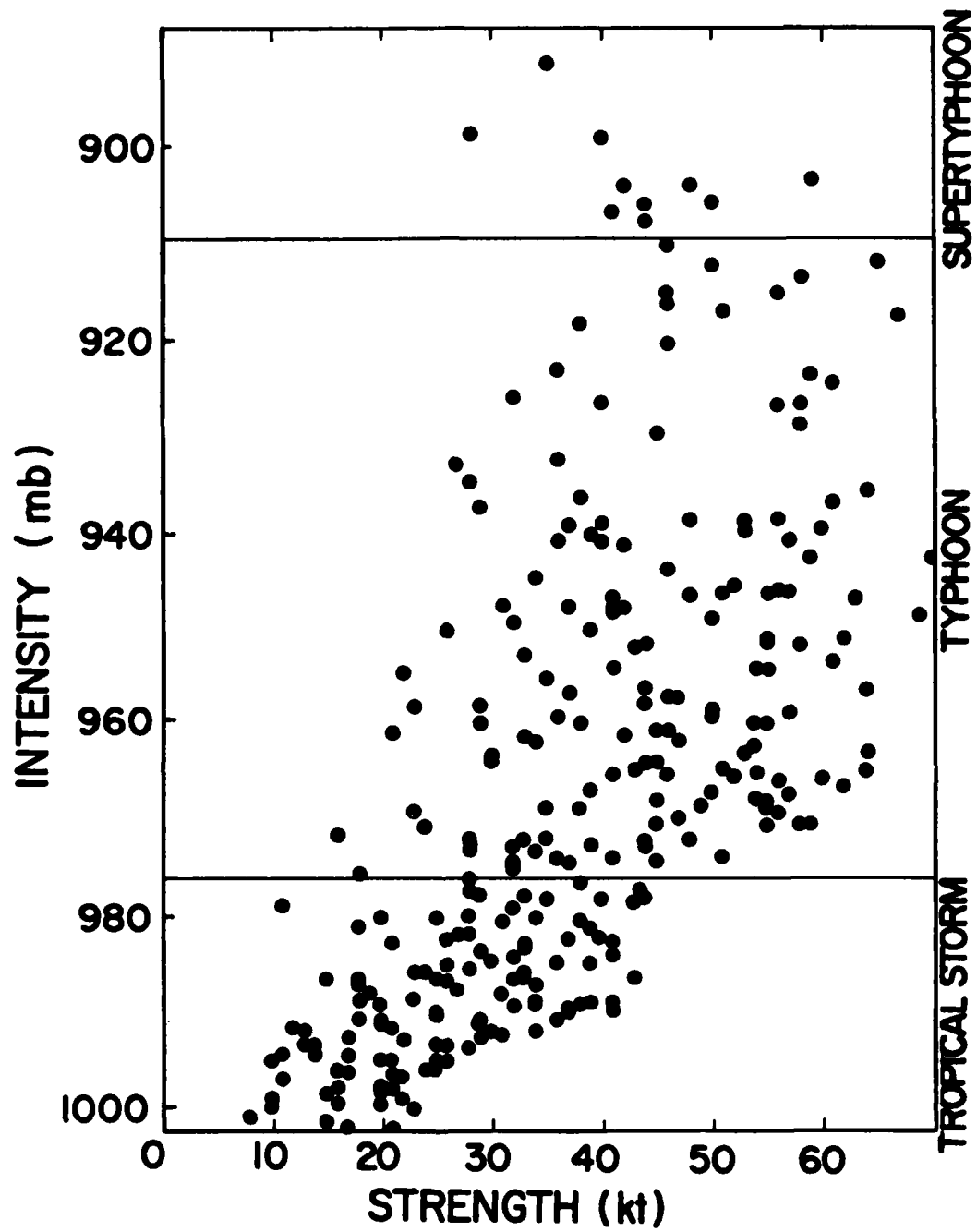
Fig. 4.1. Intensity (minimum sea-level pressure) versus strength
scatter diagram.
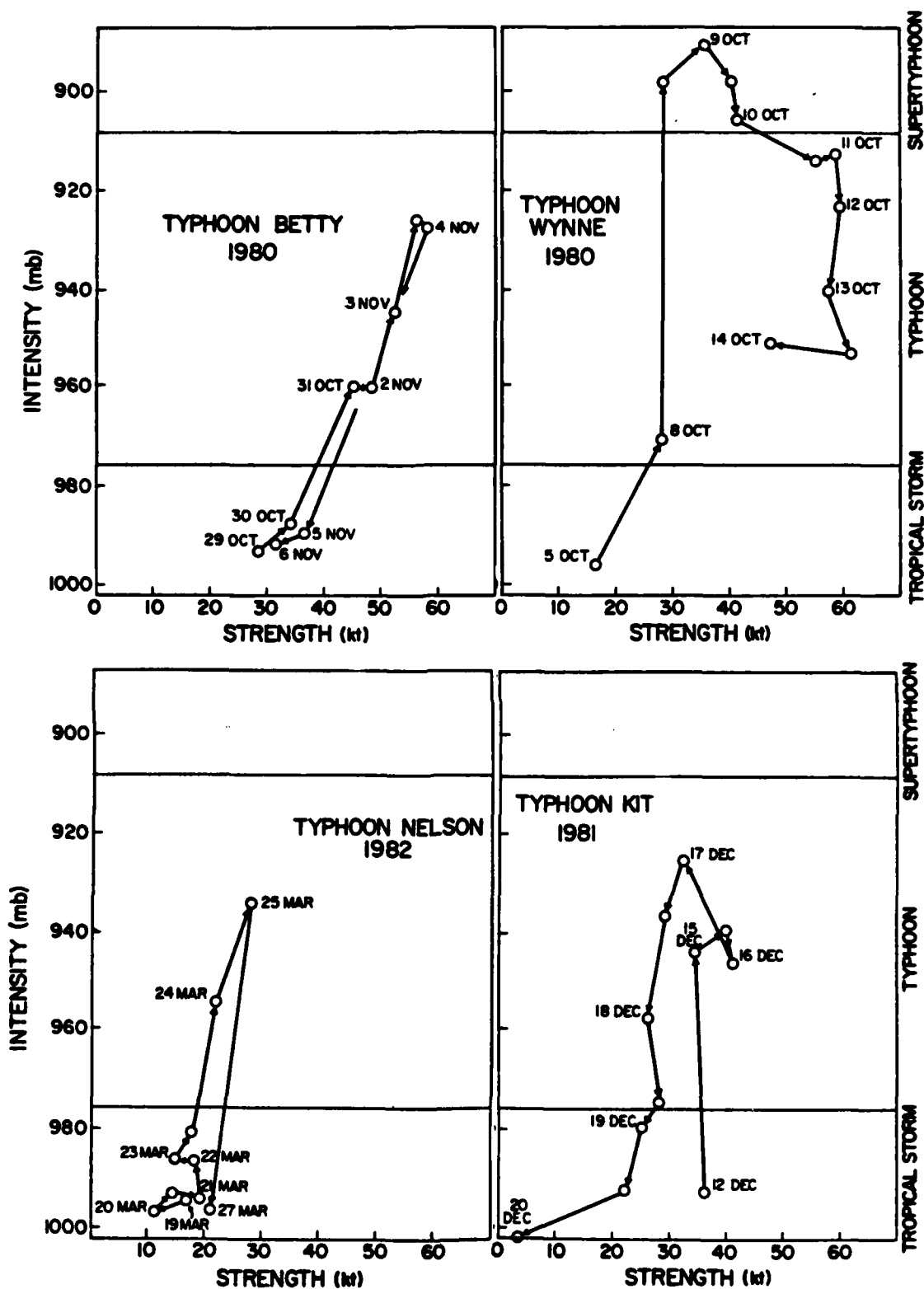
Fig. 4.2. Intensity vs. strength for Typhoons Betty, Wynne, Nelson and Kit throughout their life cycles.

increased in intensity while building its strength. After peak intensity, strength values receded along with its intensity. If all cyclones followed the example of Typhoon Betty, forecasting the wind profile would be possible simply knowing the central pressure. However, this was not the case. Supertyphoon Wynne exhibited a vastly different path. Once Wynne attained typhoon intensity, central pressure dropped sharply without a change in strength. However, as Wynne began to fill, it continued to increase in strength. Finally, for two days Wynne filled further while holding strength relatively constant. Typhoon Nelson intensified and later filled without ever exhibiting much of a change in strength. Lastly, note how Typhoon Kit began its life cycle with nearly its highest strength and continually weakened thereafer. Plotting these incremental changes in intensity and strength for all cyclones shows, in Fig. 4.3, a near zero correlation. However, further analysis showed that recurvers exhibited a decrease in intensity while increasing in strength. Therefore, intensity changes could occur independently of strength changes over a 12-hr period.

Intensity and size, whether for R-30 or R-50, exhibited similar scatter. Intensity vs. R-30, as depicted in Fig. 4.4, shows very little relationship correlating at -.60. Intensity and R-50 correlated even less at -.16 as Fig. 4.5 shows. Figure 4.6 depicts the changes in intensity against the changes in R-50, with no significant correlation between them (.05). This tenuous relationship between intensity and size implies some kind of decoupling action between the inner core of the cyclone and the region outside. In other words, changes in the inner core at times appeared to occur independently of changes elsewhere along the wind profile.
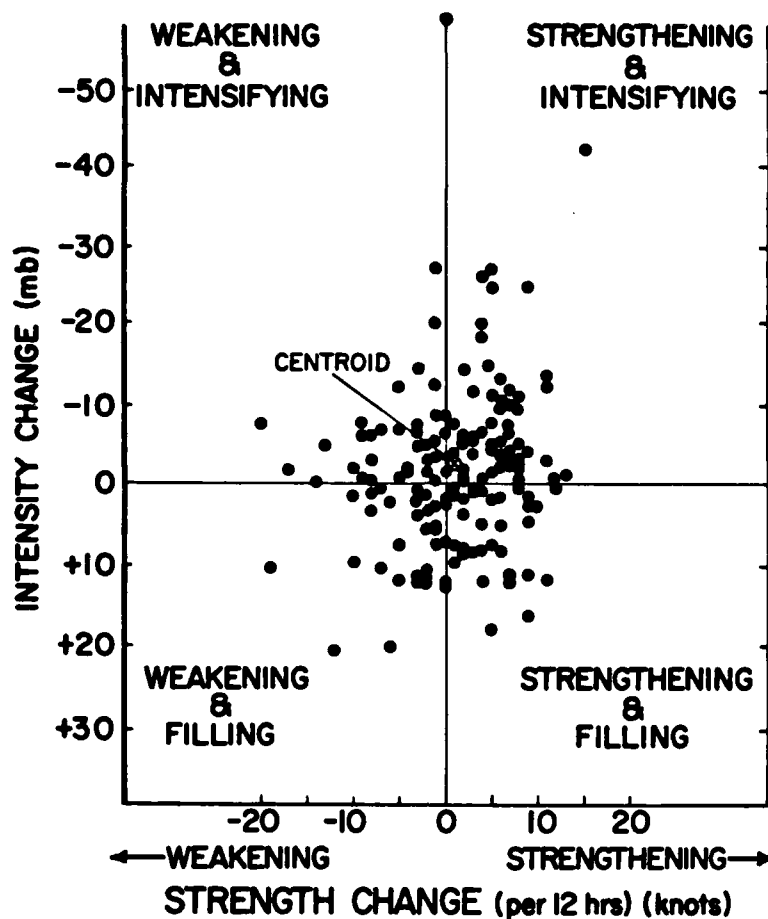
Fig. 4.3. Intensity changes (mb per 12 hours) versus strength changes
which occurred in 12 hours.

4.2 Strength vs. Size

Outside 1° radius, the wind profile did appear to respond to

forcings in a coordinated fashion. Figure 4.7 shows a strong

relationship between strength and R-30 (correlation of .9). This

powerful relationship allows strength to be estimated given the average

extent of 30-kt surface winds (35-kt flight level winds). The least-

squares best fit equation is:

$$\text{Strength} = 13.7 + .182 \ (\text{R-30})$$

or the inverse

$$\text{R-30} = -75.3 + 5.5 \ (\text{STRENGTH})$$
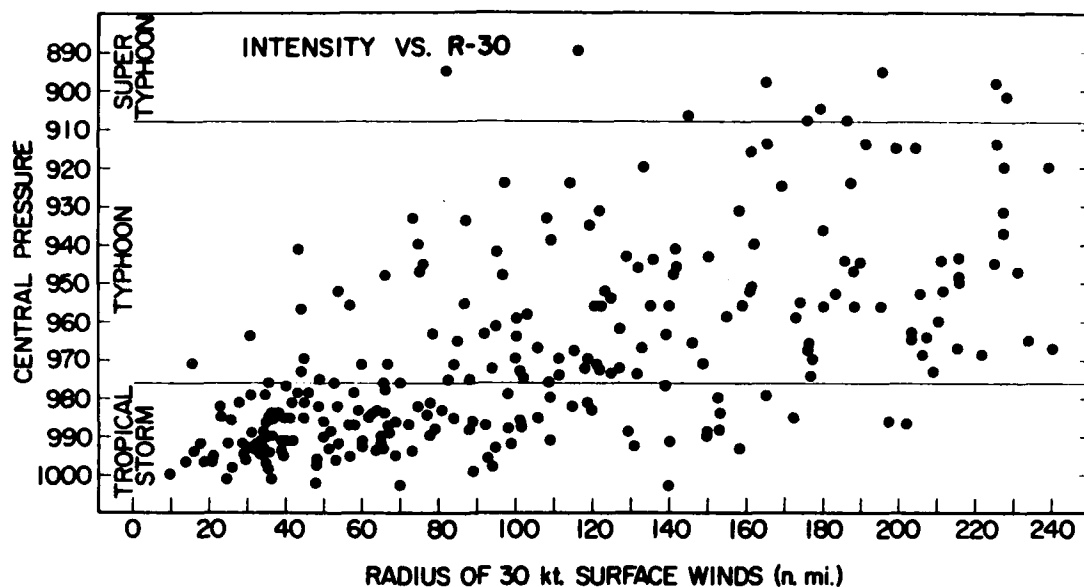
Fig. 4.4. Intensity (minimum sea-level pressure) versus the radius of
30 kt wind speeds shows large scatter.
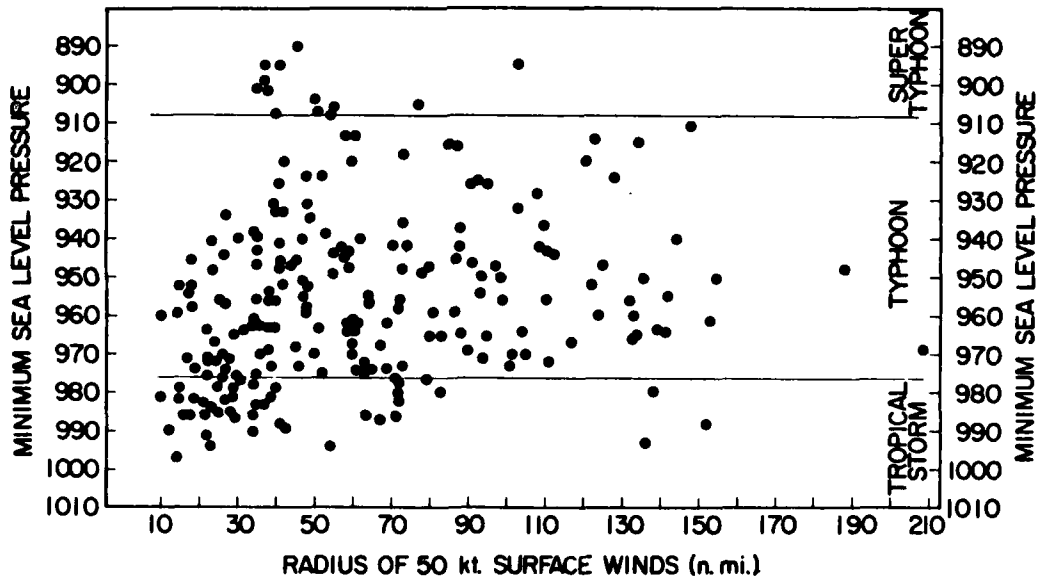
Fig. 4.5. Intensity (minimum sea-level pressure) versus the radius of
50 kt wind speed (n mi) scatter diagram.
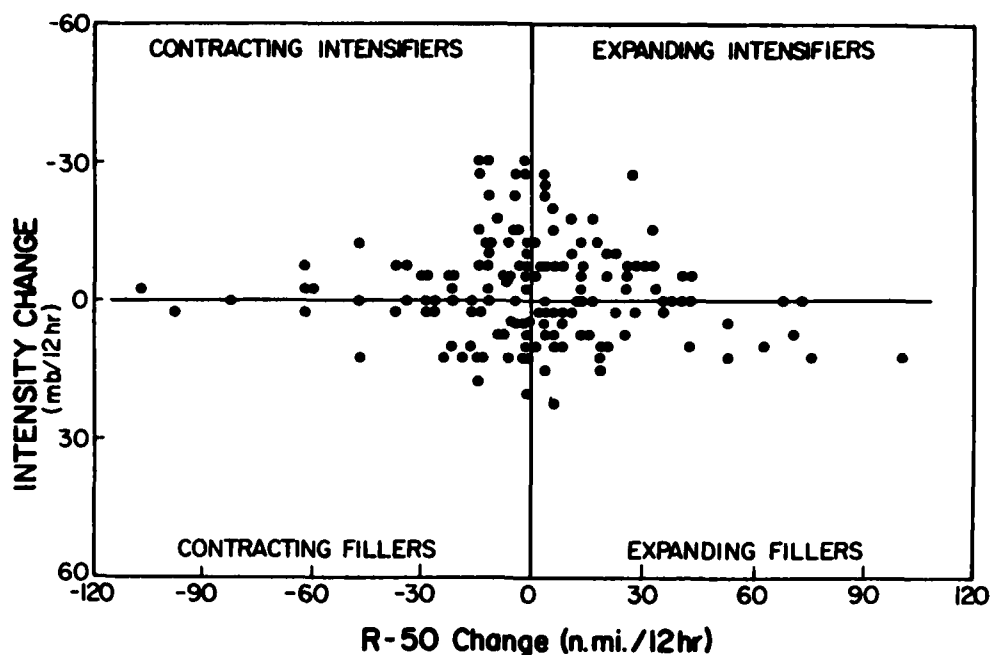
Fig. 4.6.   Intensity changes (mb/12 hours) vs. R-50 changes (n mi/12 hours).

where R-30 is expressed in n mi, and strength in knots. For example, a R-30 of 200 n mi gives a strength of 50 kt.

4.3   Size in NAT

Although all calculations presented so far have been made for 4 (or 2 beyond 150 n mi) quadrant averages in cyclone relative motion coordinates (MOT), the forecaster does not always have this all-quadrant information readily available in order to convert wind data relative to the cyclone's motion. Therefore, the above relationships were examined in cases where the farthest extent of 30-kt or 50-kt surface winds along any radial leg in the fixed (NAT) coordinate system were used. Figure 4.8 indicates, as expected, little relationship between intensity and the maximum 30-kt surface wind extent along any quadrant (correlates at -.48). Similarly, Fig. 4.9 gives the farthest radius that the 50-kt
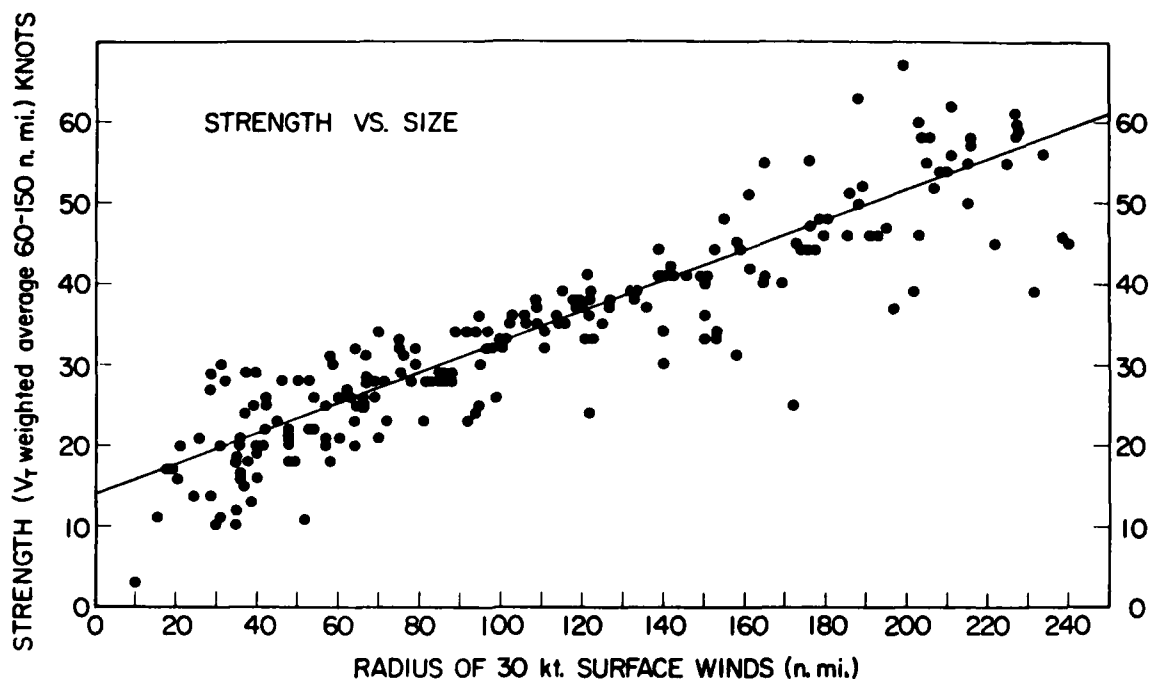
Fig. 4.7. Strength versus the radius of 30 kt surface wind speeds (35 kt at 700 mb).
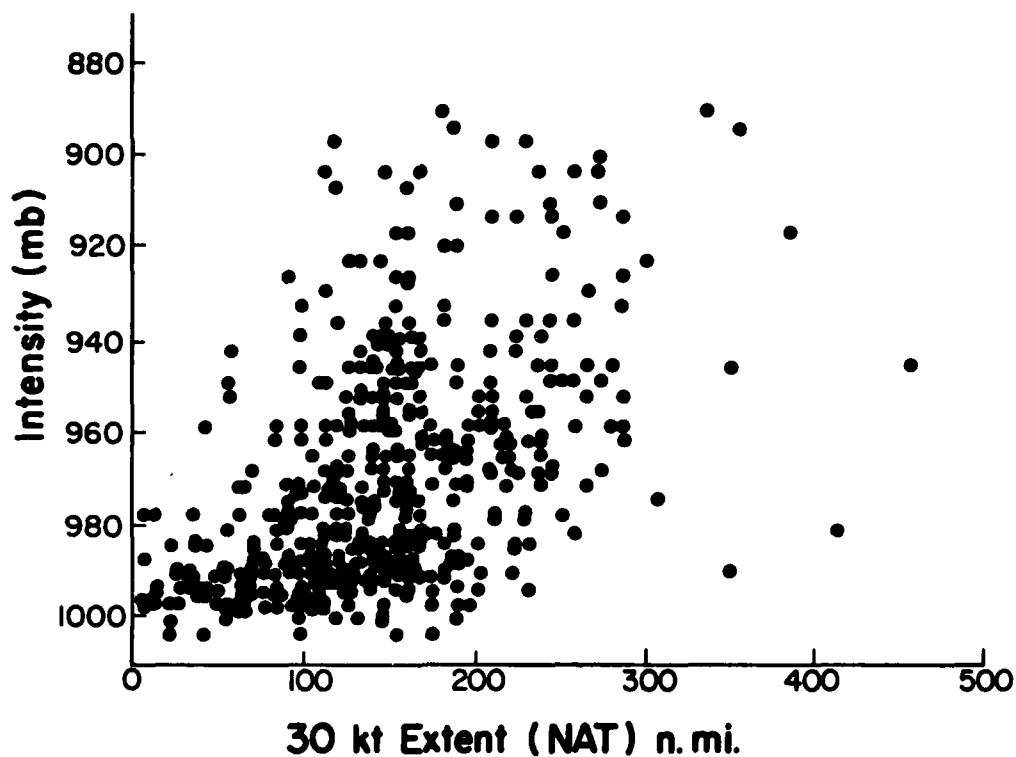
Fig. 4.8. Intensity vs. the farthest reported extent of 30-kt wind speeds for any radial leg (not averaged) for the case where motion of the cyclone center has not been subtracted out. Few data points existed outside of 250 n mi because flights tracks did not routinely extend beyond this.

48
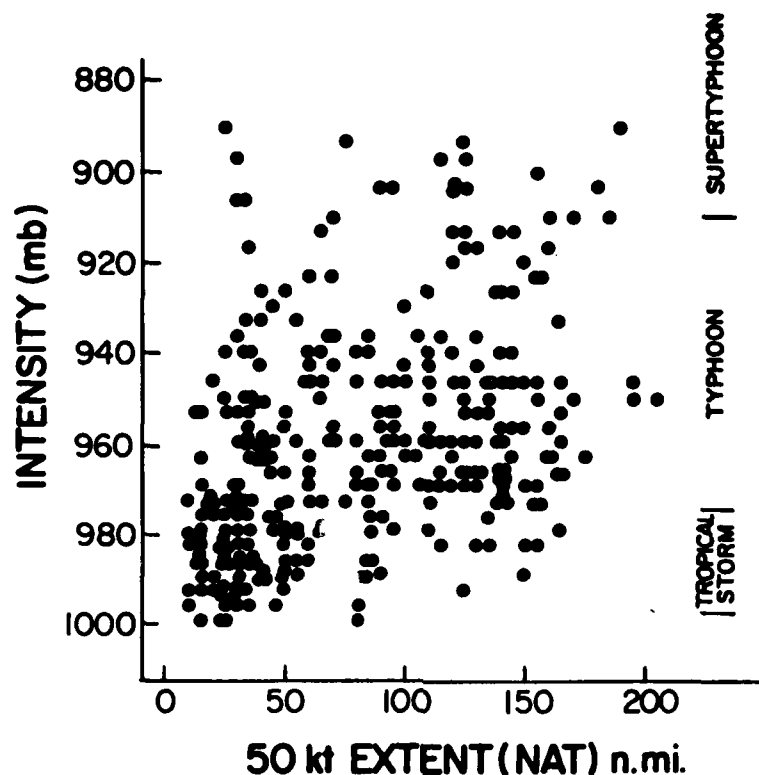
Fig. 4.9. Intensity vs. the farthest reported extent of 50-kt wind
speeds (not averaged) for any quadrant for the case where the
motion of the cyclone center was not factored in.

surface wind extends in any quadrant vs. intensity correlating at -.34.

While intensity and size did not relate well, strength and size still

did in the Natural (NAT) or fixed coordinate system. Strength and the

farthest extent of 30-kt winds correlated at .67 (shown in Fig. 4.10).

Note that for the handful of flight missions where it was possible to

sample the extent of 30-kt winds beyond 250 n mi, the farthest was found

at 450 n mi. These larger systems could certainly affect quite a large

region. Strength vs. R-50 (NAT) correlated at .79 showing a good

relationship in Fig. 4.11.

Examination of the interaction among the various regions of the

wind profile provided some interesting insights. Intensity appeared to

be, in and of itself, quite a variable feature in the tropical cyclone,
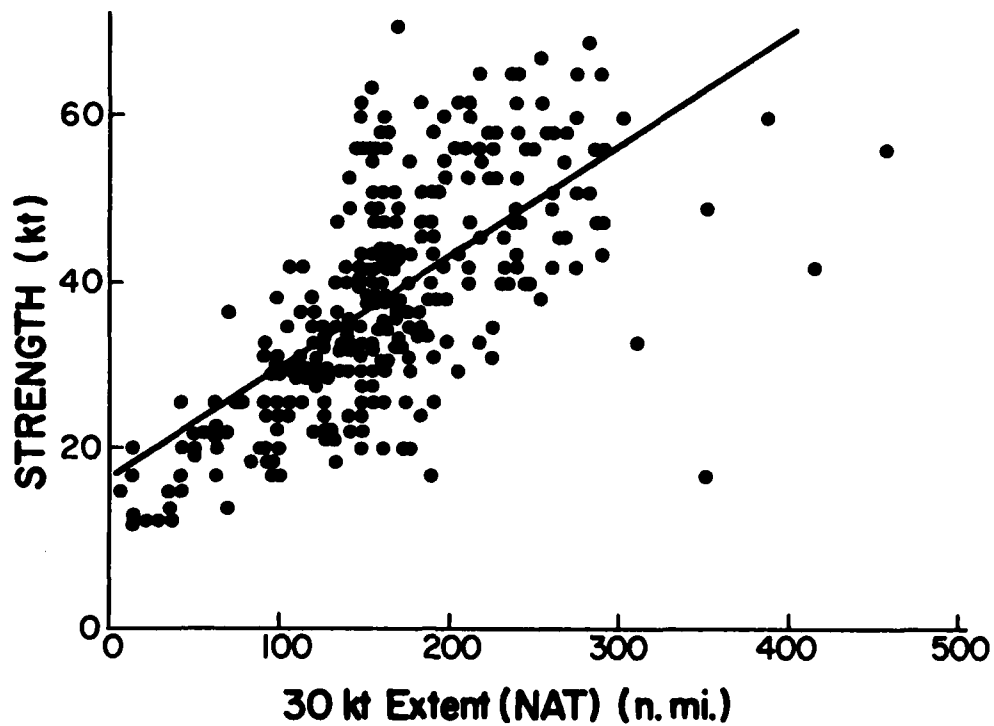
Fig. 4.10.   Strength vs. the outer limit at which 30 kt wind speeds were
            measured in NAT coordinates (cyclone motion not included).

relating poorly to strength, R-30 and R-50.   Indeed, intensity changes

over a 12-hr period appeared to occur independently of strength and size

changes.   Still, strength and R-30 related quite well.   In order to

better relate intensity vs. strength one needs to know the cyclone's eye

characteristics.   The next chapter discusses this association.

5.   THE ASSOCIATION OF THE EYEWALL WITH THE WIND PROFILE

So far, in discussing the relationships between various aspects of
the wind profile, it is evident that strength related very closely with
R-30 but not to intensity. Intensity and strength bear only a weak
relationship with each other, particularly for the most intense
cyclones. One goal of this research was to provide a method with which
to predict the wind profile given information found near the center of
the cyclone. The data presented so far indicated that this was not
possible. However, what happens to these relationships when information
on the size of the cyclone's eye is provided?

For reconnaissance reporting purposes, an eyewall was not reported
unless it subtended, on radar, at least 180 degrees of arc around the
cyclone's center. For this study, the radius from the cyclone center to
the beginning of the eyewall convection was used to determine the size
of the eye. The eyewall convection must also be distinct from the
spiralling convective bands. The eye, if it exists, was observed as the
aircraft approached the center, which was typically twice each mission.
All reports of eye radii were averaged for each mission to provide one
typical eye size. Figure 5.1 shows the distribution of the eye size by
cyclone intensity. From this figure, one can see that it was possible
to observe eyes in tropical storms as well as typhoons. In this sample,
24% of all measured tropical storms exhibited an eye. Note also that
both tropical storms and supertyphoons could exhibit a small eye. It
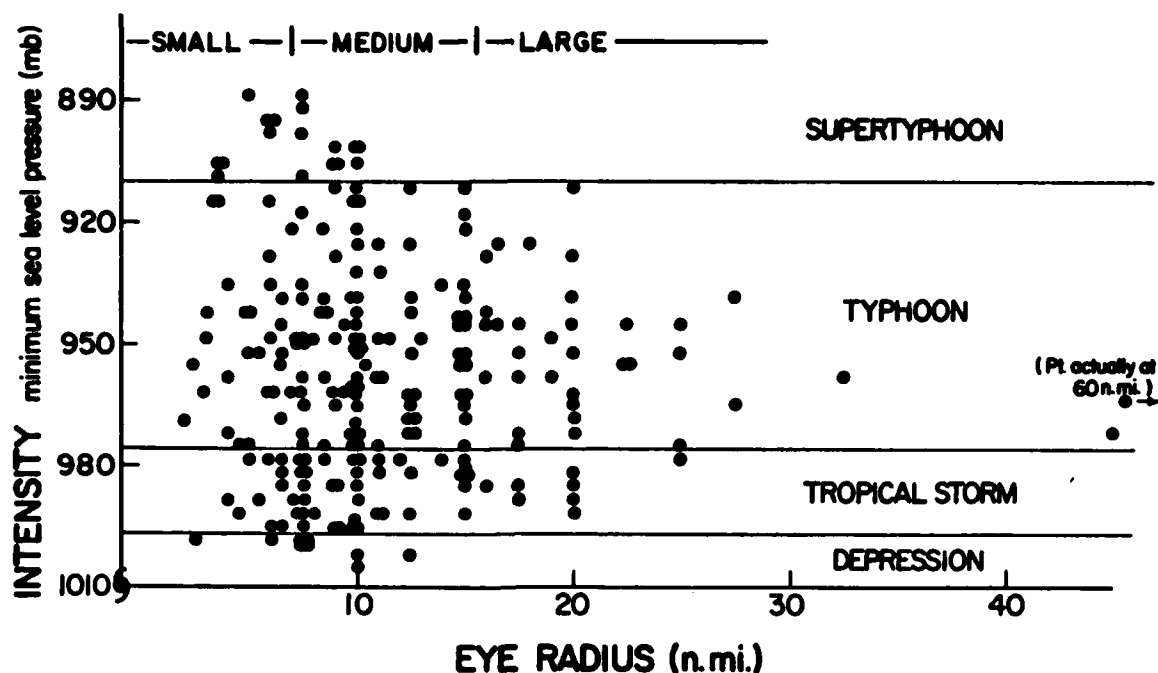
Fig. 5.1. Eye size vs. intensity.

appeared that there was no significant correlation between the size of the eye and cyclone intensity.

5.1 The Eye Classes

In order to relate the eye's size to the adjoining wind profile the eye was classified by its size. The absolute value of the eye size was of little use without this classification. Hoecker and Brier (1970) noted a $\pm$ 4 n mi fluctuation in 4 hours for the three hurricanes, Carla of 1961, Betsy of 1965 and Beulah of 1967, having studied the eye character of each continuously for 24 hours. Therefore, in order to compensate for this short-period fluctuation, eye sizes were classified into three groups: small, medium, and large. A fourth class was added for the case of the cyclone with no apparent eye. Table 5.1 defines each class. Note that 53% of all cyclones showed no eye on radar. These were mostly tropical storms, yet many were typhoons as well (29% of all typhoons did not exhibit an eye). This phenomenon of a

TABLE 5.1

Eye-class	Radius (n mi)	No. of Cases	% of Total
Small eye	2 - 7.5	79	15
Medium eye	8 - 15	122	24
Large eye	15.5 - 60	42	8
No eye		274	53

typhoon with no apparent eye was documented by Fett (1968) for the case of Typhoon Ethel which was a typhoon of 80 kt with no eye. The small-eye class comprised 15% of the data sample with radii less than 8 n mi. Typhoon Dinah exhibited the smallest radius of 2 n mi. The medium-eye class incorporated one quarter of the sample, with radii of 8 to 15 n mi. The average of this medium-eye class was 11 n mi. Finally, the large-eye class extended beyond a radius of 15 n mi. Typhoon Thad had the largest eye in the sample, 60 n mi - see Fig. 5.2.

Once separated by eye class, a much better relationship between cyclone intensity and strength was obtained. Figure 5.3 shows how an approximate straight line can be drawn for each eye class. Looking at just the cases of the small eye or no eye, Fig. 5.4 shows the difference in character along the intensity/strength path much clearer. Cyclones with similar central pressures tended to have much greater strength if no eye existed as opposed to a small eye. Similarly, cyclones of equal strength tended to be more intense the smaller the eye. The linear least squares best fit relationships between cyclone strength (ST) and intensity, given the eye class, are as follows:
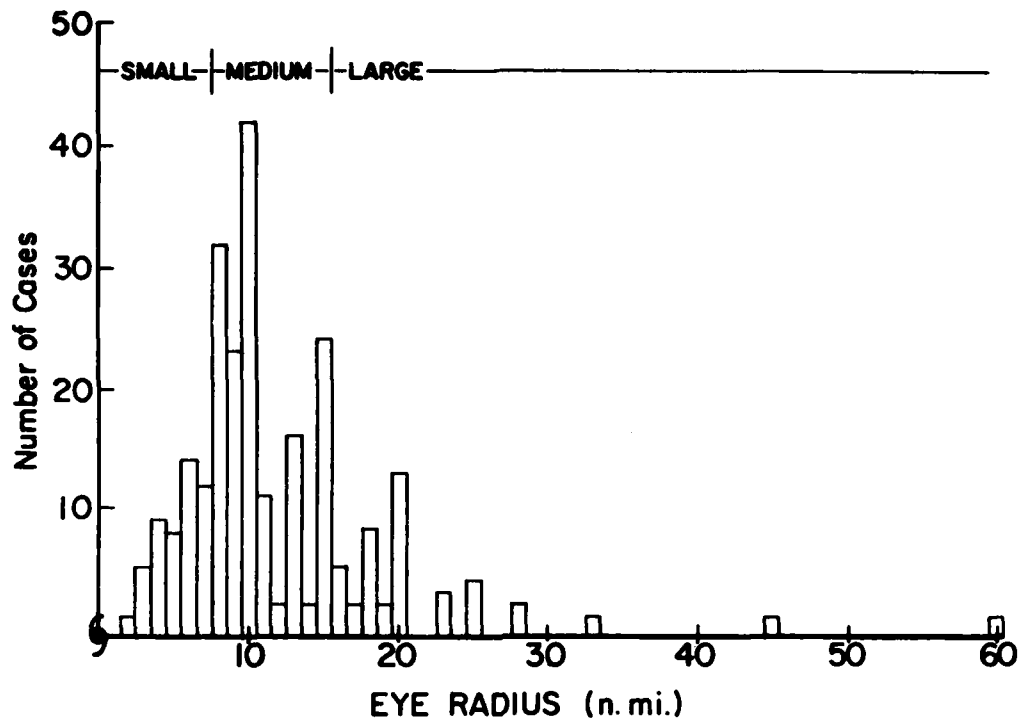
Fig. 5.2. Eye size distribution and corresponding eye classes.
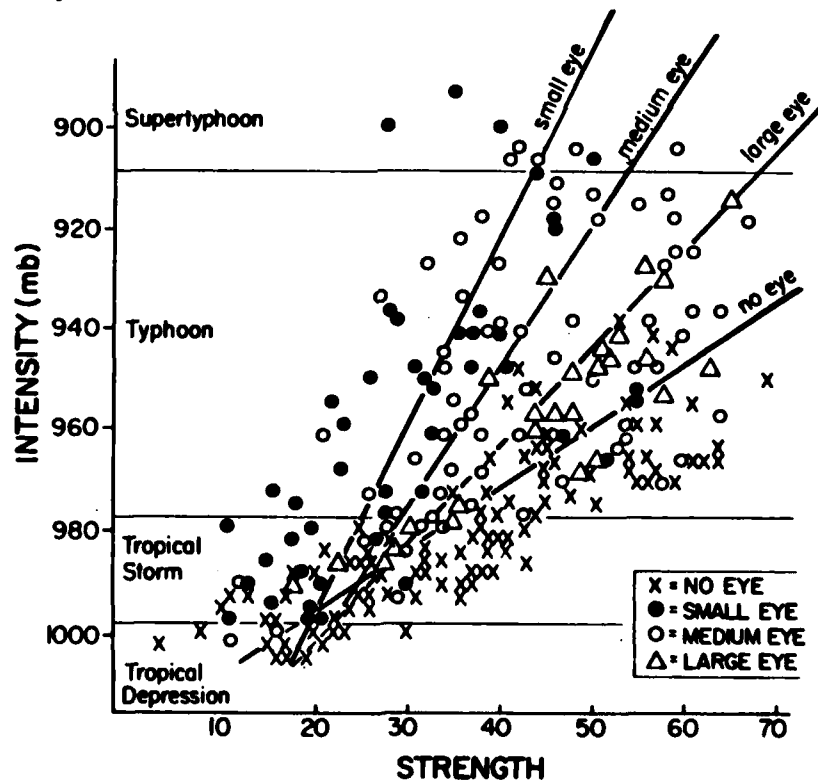
Fig. 5.3. Intensity versus strength differs by eye class (small eye 0–
7.5 n mi; medium eye 7.5–15 n mi; large eye 15–60 n mi).
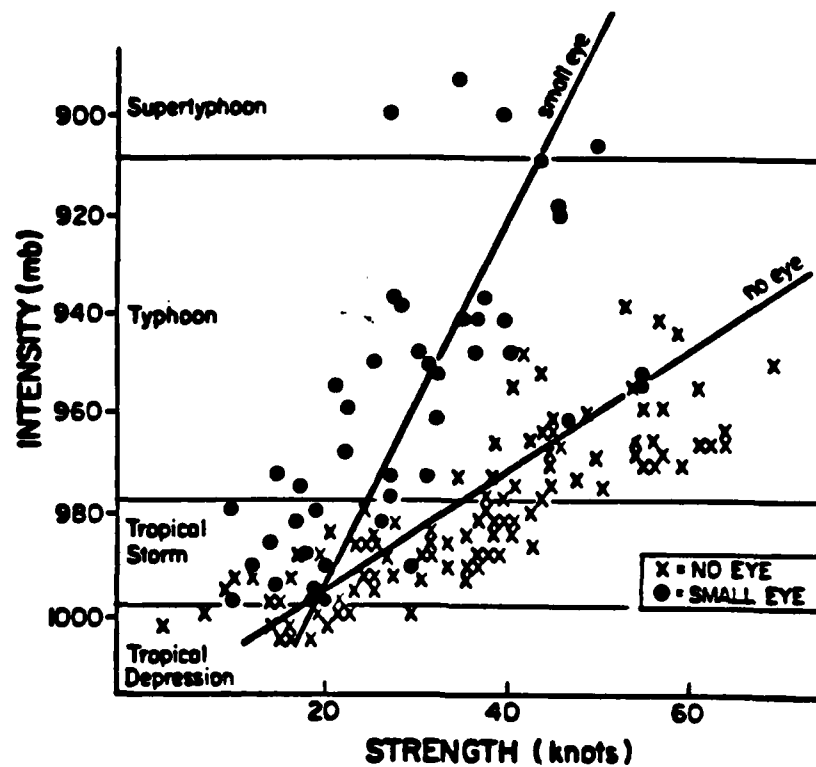
Fig. 5.4.   Intensity versus strength for the small eye class and no eye class.

Small eye: $ST = 321 - .303 \, (SLP_{min})$

Medium eye: $ST = 361 - .337 \, (SLP_{min})$

Large eye: $ST = 536 - .513 \, (SLP_{min})$

No eye: $ST = 837 - .818 \, (SLP_{min})$

where ST = Strength measured in kt

SLP_{min} = minimum sea level pressure (mb)

For example, given a central pressure of 976 mb the cyclone without an eye would have an average strength of 39 kt, while that with a small eye would average a strength of 25 kt.

Each cyclone, once separated by its eye class, exhibited characteristic properties along the wind profile.   Table 5.2 is a

TABLE 5.2

Average parameters of intensity, strength, R-30, and intensity change, for the 1980-82 data set partitioned by eye class.

AVERAGES BY EYEWALL DIAMETER

	INTENSITY (mb)	STRENGTH (knots)	R-30 (n. mi.)	INTENSITY CHANGE (mb-12hrs)
No Eyewall	985 mb	34 kt	93 n. mi.	±5 mb
◯ Large Eye (>15 n.mi.)	957 mb	47 kt	145 n. mi.	±8 mb
◯ Medium Eye (8-15 n.mi.)	956 mb	40 kt	117 n. mi.	±9 mb
○ Small Eye (2-7.5 n.mi.)	954 mb	33 kt	89 n. mi.	±12 mb

compilation of each eye class providing the average intensity, strength, R-30 and intensity change (per 12 hours). The cyclone without an eye was, on average, a tropical storm (985 mb approximates a 53-kt maximum wind using the Atkinson/Holliday fit). The cyclone with an eye had an intensity of about 956 mb regardless of whether the eye was small, medium or large. Note that the larger the eye, the greater the strength and larger the extent of 30-kt surface winds. Furthermore, the smaller the eye, the more rapidly changes occurred in intensity. The cyclone with a small eye fluctuated in intensity over twice the amount of the cyclone without an eye. Also note that the kinetic energy of small eye cyclones in their strength region (1 to 2.5° radius) is less than half that of the large eye cyclones even though their central pressures are

the same.

5.2 Average Wind Profiles

The concepts of cyclone intensity, strength, and size provided a means to quantify varying regions of the wind profile. To qualitatively view the wind profile as the eye character changes, average profiles were obtained for each eye and intensity class. Figure 5.5 (a through l) shows examples of typical wind profiles for each intensity and eye class and also includes the range of the standard deviation. For instance, in Fig. 5.6a twenty cases of tropical storms with small eyes were averaged to yield this profile. On the average, the intensity of the tropical storm with a small eye was 985 mb, maximum wind observed at flight level was 54 kt and strength 19 kt. The tropical storm with no apparent eye exhibited an intensity, on the average, of 987 mb, maximum wind of 53 kt and strength of 31 kt. Note that although the intensities of the tropical storm with a small eye or without an eye were quite similar, their strengths were quite different. The two-sample t-test indicates a 99.97% confidence level that they are, in fact, significantly different. These profiles provide a quick look at the structure of the wind profile given information found only near the center, i.e., size of the eye and central pressure.

At present (JTWC, 1984), radii of 30-kt and 50-kt surface wind speeds are estimated by the forecasters at JTWC using Holland's 1980 wind/pressure scheme. No regard is given to the size of the eye. Since this is the first observational study of the wind profile incorporating wind measurements as far out as 250 n mi from the center, the differences in R-30 between a small eye minimal typhoon and a minimal typhoon without an eye are believed to be valid. The student's t-test

TROPICAL STORM w/ Small Eye count 20

SLP (min)	985 mb
MAX WIND	54 kt
STRENGTH	19 kt
EYE RADIUS	7 n. mi.

R-30 at 34 n.mi.

a

TROPICAL STORM w/ Medium Eye count 23

SLP (min)	986 mb
MAX WIND	55 kt
STRENGTH	25 kt
EYE RADIUS	11 n. mi.

R-30 at 41 n. mi.

b
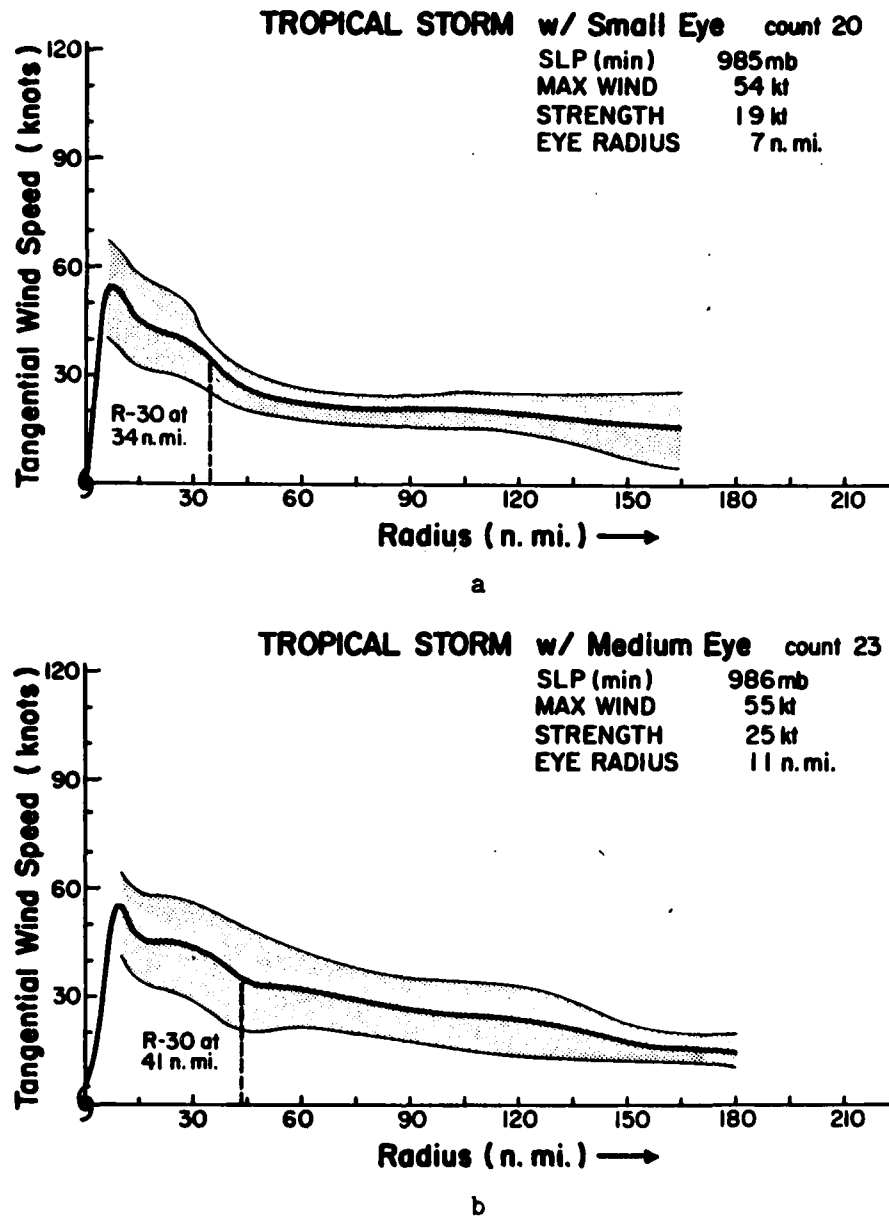
Fig. 5.5.   Average wind profiles show mean position and standard
deviation (stippled area) with average intensity, strength
and eye radius for the cases of tropical storms with: (a)
small eye, (b) medium eye, (c) no eye, (d) minimal typhoons
with small eye, (e) medium eye, (f) large eye, (g) no eye,
(h) intermediate typhoons with small eye, (i) medium eye, (j)
large eye, and (k) extreme typhoons with small eye, and (l)
medium eye.

TROPICAL STORM w/ no eye   count 80
SLP (min)
MAX WIND   53 kt
STRENGTH   31 kt

R-30 at 58 n. mi.

Tangential Wind Speed (knots)

Radius (n. mi.) ⟶

c

MINIMAL TYPHOON   w/ Small Eye   count 15
SLP (min)   963 mb
MAX WIND   80 kt
STRENGTH   86 kt
EYE RADIUS   6 n. mi.

R-50 at 13 n. mi.

R-30 at 101 n. mi.

Tangential Wind Speed (knots)

Radius (n. mi.) ⟶

d

Fig. 5.5.   Continued.

MINIMAL TYPHOON   w/ Medium Eye   count 34

SLP (min)	963 mb
MAX WIND	79 kt
STRENGTH	40 kt
EYE RADIUS	11 n. mi.

R-50 at 28 n. mi.

R-30 at 165 n. mi.

Tangential Wind Speed (knots)

Radius (n. mi.) ⟶

e

MINIMAL TYPHOON (976-950 mb)   **w/ Large Eye   count 15**

SLP (min)	962 mb
MAX WIND	81 kt
STRENGTH	47 kt
EYE RADIUS	26 n. mi.

R-50 at 68 n. mi.

R-30 at 145 n. mi.

Tangential Wind Speed (knots)

Radius (n. mi.) ⟶

f

Fig. 5.5.   Continued.

MINIMAL TYPHOON   w/ No Eye   count 45

SLP (min)   965 mb
MAX WIND   75 kt
STRENGTH   49 kt

R-50 at 90 n. mi.

R-30 at 220 n.mi.

Tangential Wind Speed (knots)

Radius (n. mi.) ⟶

g

INTERMEDIATE TYPHOON   w/Small Eye   count 14
(950–920 mb)

SLP (min)   940 mb
MAX WIND   93 kt
STRENGTH   34 kt
EYE RADIUS   6 n.mi.

R-50 at 35 n.mi.

R-30 at 107 n.mi.

Tangential Wind Speed (knots)

Radius (n. mi.) ⟶

h

Fig. 5.5. Continued.

INTERMEDIATE TYPHOON (950-920 mb) w/Medium Eye   count 27

SLP (min)   938 mb
MAX WIND   95 kt
STRENGTH   48 kt
EYE RADIUS   12 n. mi.

R-50 at 70 n. mi.
R-30 at 192 n. mi.

i

INTERMEDIATE TYPHOON (950-920 mb) w/Large Eye   count 14

SLP (min)   939 mb
MAX WIND   97 kt
STRENGTH   54 kt
EYE RADIUS   19 n. mi.

R-50 at 76 n. mi.
R-30 at 209 n. mi.

j

Fig. 5.5. Continued.

EXTREME TYPHOON w/ small eye   count 13
(920-890 mb)

SLP (min)	906 mb
MAX WIND	107 kt
STRENGTH	45 kt
EYE RADIUS	5 n. mi.

Tangential Wind Speed (knots)

R-50 at 47 n. mi.

R-30 at 185 n. mi.

Radius (n. mi.) ⟶

k

EXTREME TYPHOON   w/ Medium Eye count 11
(920-890 mb)

SLP (min)	908
MAX WIND	115 kt
STRENGTH	50 kt
EYE RADIUS	10 n. mi.

Tangential Wind Speed (knots)

R-50 at 63 n. mi.

R-30 at 203 n. mi.

Radius (n. mi.) ⟶

l

Fig. 5.5. Continued.

SMALL EYE

	SLP (mb)	Strength (kt)
Tropical Storm	985 mb	19 kt
Minimal Typhoon	963 mb	36 kt
Intermediate	940 mb	34 kt
Extreme	906 mb	45 kt

Extreme Typhoon (920-890mb)

Intermediate Typhoon (950-920mb)

Minimal Typhoon (976-950mb)

Tropical Storm (997-976mb)

Tangential Wind Speed (knots) vs Radius (n. mi.)

a

MEDIUM EYE

	SLP (mb)	Strength (kt)
Tropical Storm	986 mb	25 kt
Minimal Typhoon	963 mb	40 kt
Intermediate	938 mb	48 kt
Extreme	908 mb	50 kt

Extreme (920-890mb)

Intermediate

Minimal Typhoon (976-950mb)

Tropical Storm (997-976mb)

Tangential Wind Speed (knots) vs Radius (n. mi.)

b

Fig. 5.6. Average wind profiles by eye class giving average intensity and strength for cyclones with: (a) small eyes, (b) medium eyes, (c) large eyes, and (d) no eyes.

LARGE EYE

	SLP (mb)	Strength (kt)
Minimal Typhoon	962 mb	47 kt
Intermediate Typhoon	939 mb	54 kt

Tangential Wind Speed (knots)

120

90

60

30

Intermediate Typhoon (950-920mb)

Minimal Typhoon (976-950mb)

30 60 90 120 150 180 210

Radius (n. mi.) ⟶

c

NO EYE

	SLP (mb)	Strength (kt)
Tropical Storm	987 mb	31 kt
Minimal Typhoon	965 mb	49 kt

Tangential Wind Speed (knots)

120

90

60

30

Minimal Typhoon

Tropical Storm

30 60 90 120 150 180 210

Radius (n. mi.) ⟶

d

Fig. 5.6. Continued.

revealed that they were significantly different at the 99.98% confidence level. This relationship should enable the forecaster to better estimate the radius of a particular wind speed given the eye class and central intensity of the cyclone.

Figure 5.6 (a through d) compares the varying wind profiles of different intensity separated by eye class. For the cases within the small-eye class, Fig. 5.6a shows a common peak close in to the center as is expected, and a rapid drop away from this peak. On the other hand, figure 5.6c shows that the large-eye cases exhibit a more gradual reduction in wind speed outside the maximum wind zone.

Finally, to further examine the association of the eye on the wind profile, Fig. 5.7 (a through d) divides each averaged profile by intensity class. The minimal typhoon was the only class to include representatives of all four eye classes. Looking at Fig. 5.7b, note that all four eye classes have similar central pressures and similar maximum wind speeds. The difference lies in the strength, with values ranging from 36 kt for the small eye to 49 kt for the case without an eye. In terms of the kinetic energy in the region of strength, the case of no eye has nearly twice the kinetic energy of the cyclone with a small eye. This has direct application to total rainfall of the cyclone, total areal extent of gale force winds and storm surges, and other cyclone features.

TROPICAL STORMS (997-976 mb)

	SLP	Max Wind	Strength
No Eye	987 mb	53 kt	31 kt
Medium	986 mb	55 kt	25 kt
Small	985 mb	54 kt	19 kt

a

MINIMAL TYPHOON (976 - 950 mb)

Averages

	SLP (mb)	Max Wind	Strength
No Eye	965	75 kt	49 kt
Large	962	81 kt	47 kt
Medium	963	79 kt	40 kt
Small	963	80 kt	36 kt
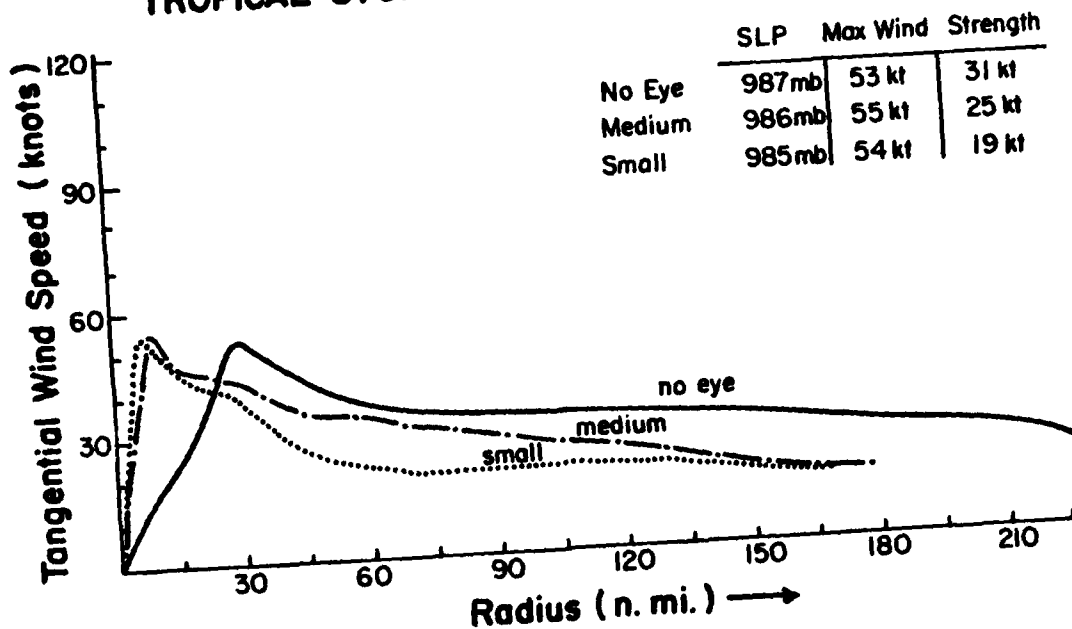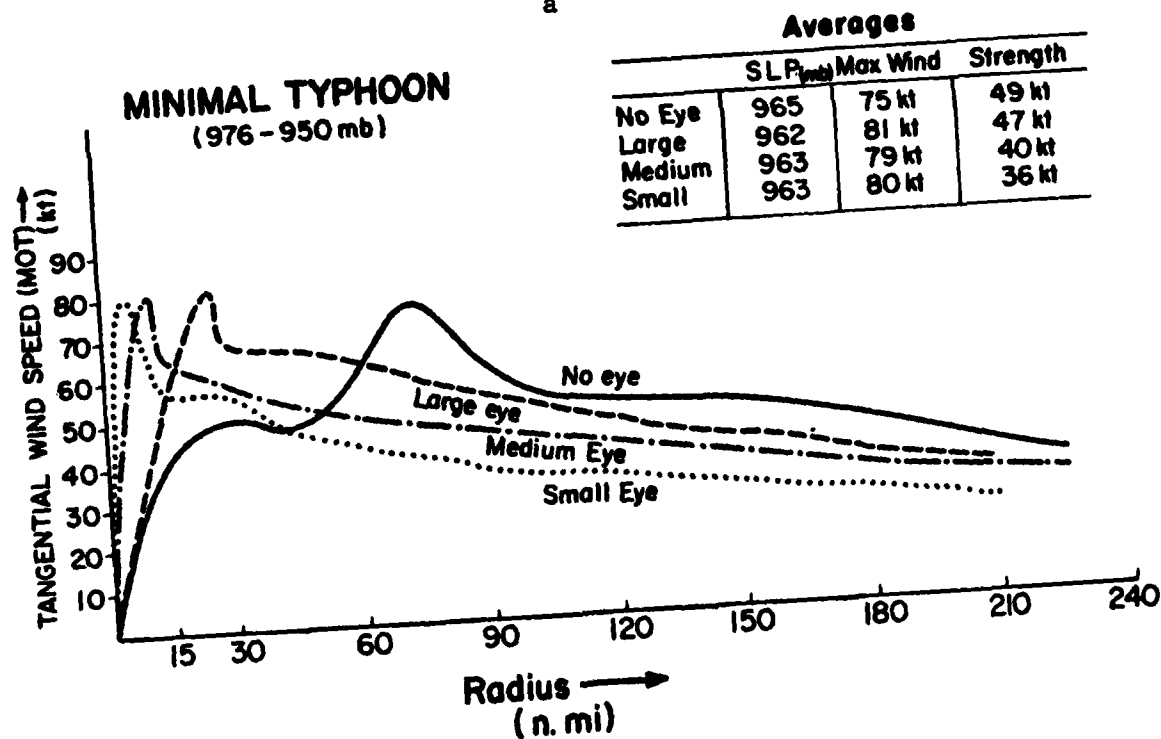
b

Fig. 5.7. Average wind profiles by intensity class shows how different the profiles can be given the eye class for: (a) the tropical storm, (b) the minimal typhoon, (c) the intermediate typhoon and (d) the extreme typhoon.

INTERMEDIATE TYPHOON (950-920mb)

	SLP	Max Wind	Strength
Large	939 mb	97 kt	54 kt
Medium	938 mb	95 kt	48 kt
Small	940 mb	93 kt	34 kt

Tangential Wind Speed (knots)

large eye

medium eye

small eye

Radius (n. mi.) ⟶

c

EXTREME TYPHOON (920-890mb)

	SLP	Max Wind	Strength
Medium	908 mb	115 kt	49 kt
Small	906	107 kt	45 kt

Tangential Wind Speed (knots)

medium

small

Radius (n. mi.) ⟶

d
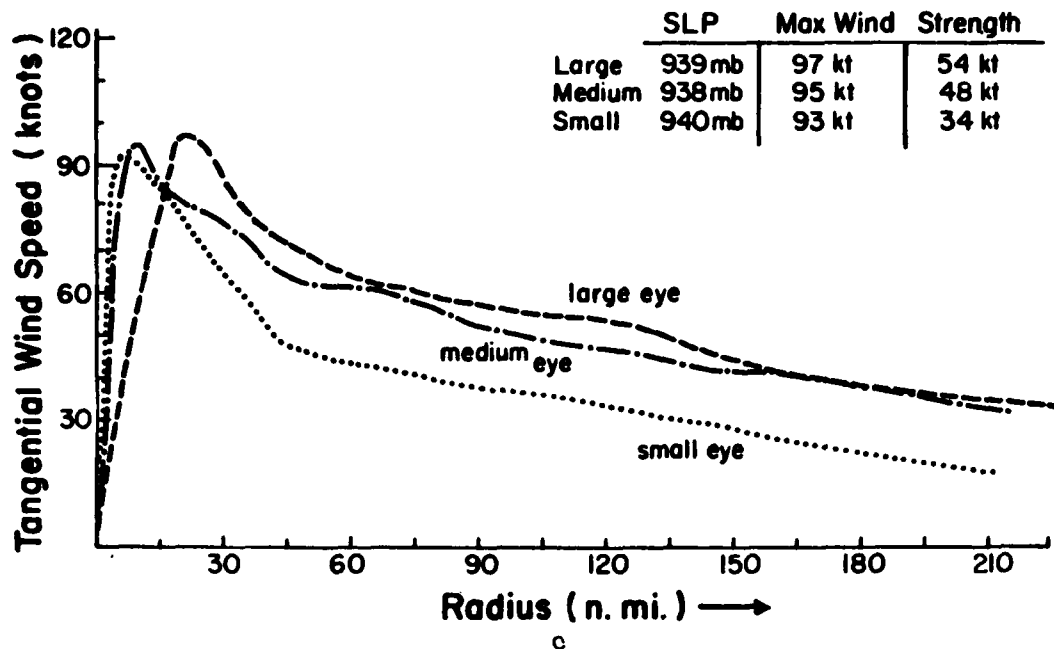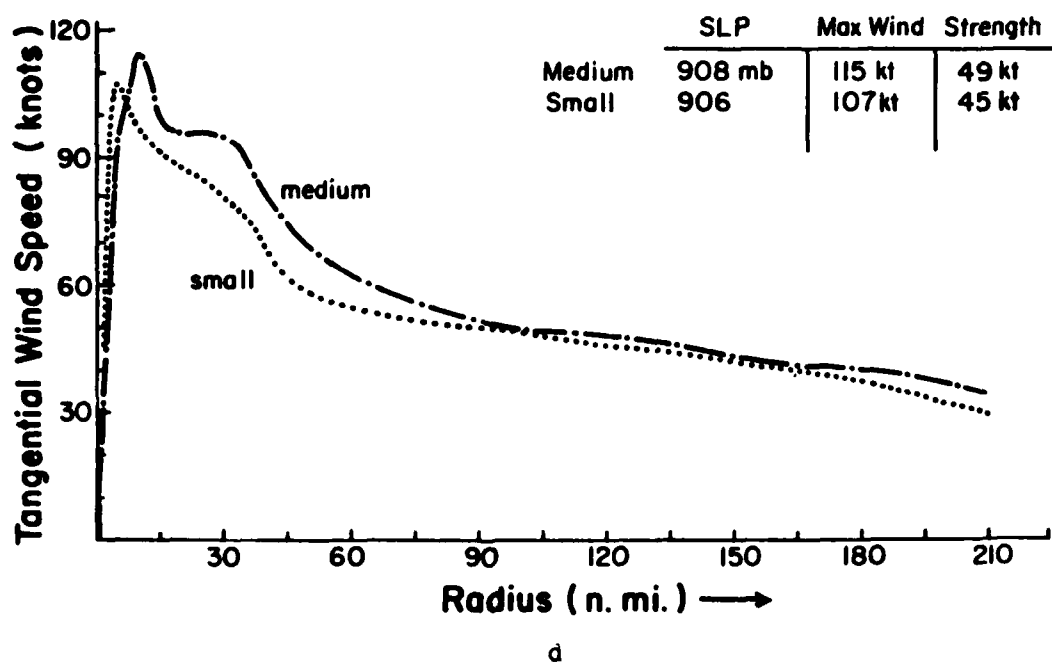
Fig. 5.7. Continued.

6. CONCLUSION

A tropical cyclone's intensity, strength and size can be used to describe its low-level wind field. Until now strength has not been available. Without a strength measure it is, at best, speculation as to what links the inner core region with its outer region. Therefore outer strength was devised to describe the wind profile lying between the core intensity and outer size. It has been shown here that intensity and strength contain many different properties producing many different effects. The core intensity of the cyclone reflects its most powerful, albeit concentrated, wind force. The outer strength of the cyclone, encompassing a larger area, reveals additional properties of the cyclone: outer strength must exert a significant influence on storm surges and its total destructive effect on coastline structures; the greater the outer strength the more moisture is drawn into the cyclone over a very large area and the more evaporation which occurs. This contributes to a broader region of rainfall; and the cyclone's net kinetic energy must increase with increased strength.

The first step of this research was to statistically examine the behavior of the cyclone's intensity, strength and size with respect to latitude, season, time of day and cyclone motion using a heretofore unresearched flight data base. Results indicated that recurving cyclones tend to strengthen while losing intensity. Cyclone intensity attained maximum values from 12° to 24°N (where the cyclones of supertyphoon intensity resided). Tropical cyclones attained their

maximum core intensity (890 mb), outer strength (70 kt) and size (beyond 250 n mi) from July to October. Diurnally, there are no noticeable changes in wind structure. Cyclone motion appeared to have a relationship with intensity far more than it does to strength or size. A cyclone was most likely to reach its highest intensities when heading west to northwest and when traveling an average speed near 10 kt.

The second step of this study focused on the 12-hour changes in intensity, strength, and size. Although tropical cyclones on the average were found to change 7 mb each 12 hours, individual intensity changes were found to reach values as high as 59 mb/12 hrs. Strength typically changed by 5 kt/12 hours but could change by as much as 15 kt over a 12-hr period. Similarly, the region of over 50-kt wind speeds could, as dramatically demonstrated by Typhoon Owen, areally increase eight-fold in 12 hours. Still, the normal fluctuation in R-50 was 22 n mi in 12 hours.

Finally, the various regions representing the wind profile, i.e., core intensity, outer strength, and size, were compared to each other in order to reveal trends. It was shown that outer strength and the domain of R-30 correlated very highly (.90). Therefore, it would appear that given the average extent of 30-kt surface winds, outer strength could be reliably predicted. Core intensity, on the other hand, was a far more variable feature. However, given the radius of the cyclone's eye or the fact that no eye existed, core intensity could be found to be a highly reliable measure of outer strength or size. Thus, the eye appears to be the link in the structure of the wind profile from the core to its outer regions. This can provide the forecaster with a very useful estimate of the entire wind profile given information found only near the center of

the cyclone (i.e., central pressure and eye class).

It is expected that these relationships which have been derived for the northwest Pacific Ocean will also prove to be generally valid for the ocean basins. It is hoped that the data of this paper will be useful to the operational forecaster.

7. FUTURE RESEARCH

There is much research to be done with this flight data. The asymmetries of the wind must be addressed. Environmental interactions on the cyclone must be sorted out. Additionally, there are typical life-cycle patterns from tropical depression to supertyphoon which need to be better documented. Finally, how does the tropical cyclone's wind profile respond when the eye's size is changing?

Although the cyclones studied here were viewed in a symmetric sense, e.g. all quadrants were averaged to provide a mean wind profile, it is recognized that maximum winds, strength, and size have pockets of greater magnitude. These are quite important for the forecaster to recognize. Further study must be able to relate central features not only to an average strength and size but also to the asymmetries as influenced by the surrounding environmental flow field.

What about the changes between cyclones? Which forcings act on some cyclones to allow maximum intensity, strength, or size values while inhibiting others? Herein lies the key to predicting the character of a single cyclone throughout its life cycle. Much more research on the factors influencing individual cases is needed.

Finally, what is it about the eye that allows it to appear in some tropical storms while remaining absent in other typhoons? Furthermore, once present, what forces the eye to contract or expand, thereby changing the nature of the wind profile?

ACKNOWLEDGEMENTS

REFERENCES

Akima, Y., 1970: A new method of interpolation and smooth curve fitting based on local procedures. *J. Assoc. Comput. Mach.*, 17, 589-602.

Anthes, R. A., 1974: The dynamics and energetics of mature tropical cyclones. *Rev. of Geoph. and Space Physics*, 12, 495-521.

Anthes, R. A., 1982: *Tropical Cyclones: Their Evolution, Structure and Effects*. American Meteorological Society, 192 pp.

Atkinson, G. D. and C. R. Holliday, 1977: Tropical cyclone minimum sea level pressure maximum sustained wind relationship for the western North Pacific. *Mon. Wea. Rev.*, 105, 421-427.

Black, P. G., H. V. Senn and C. L. Courtright, 1972: Airborne radar observations of eye configuration changes, bright band distribution and precipitation tilt during the 1969 multiple seedings of Hurricane Debbie. *Mon. Wea. Rev.*, 100, 208-217.

Colon, J. A., 1963: On the evolution of the wind field during the life cycle of tropical cyclones. NHRP Report No. 65, 36 pp.

Colon, J. A., 1964: On the structure of Hurricane Helene (1958). NHRP Rept. No. 72, 50 pp.

Colon, J. A., and Staff, NHRP, 1961: On the structure of Hurricane Daisy (1958). NHRP Rept. No. 48, 102 pp.

Dunn, G. E., and B. I. Miller, 1964: *Atlantic Hurricanes*. Louisiana State Univ. Press, 368 pp.

Dunnavan, G. M., 1983: An evaluation of 700 mb aircraft reconnaissance data for selected northwest Pacific tropical cyclones. MS thesis Naval Postgraduate School, Monterey, CA, 92 pp.

Fett, R. W., 1968: Some unusual aspects concerning the development and structure of Typhoon Billie - July 1967. *Mon. Wea. Rev.*, 96, 637-648.

Frank, W. M., 1977: The structure and energetics of the tropical cyclone I. Storm structure. *Mon. Wea. Rev.*, 105, 1119-1135.

Frank, W. M., 1984: Composite analysis of the core of Hurricane Frederick 1979. *Mon. Wea. Rev.*, 112, 2401-2420.

Frank, W. M., and W. M. Gray, 1980: Radius and frequency of 15 m/s (30 kt) winds around tropical cyclones. J. Appl. Meteor. 19 219-223.

Fritsch, F. N., and R. E. Carlson, 1980: Monotone piecewise cubic interpolation, SIAM J. NUMER. ANAL. 17, 238-246.

Fritsch, F.N., and Butland, 1980: An improved monotone piecewise cubic interpolation algorithm, LLNL Preprint UCRL-85104.

Gray, W. M., 1962: On the balance of forces and radial accelerations in hurricanes. Quart. J. Roy. Meteor. Soc., 88, 430-458.

Gray, W. M., 1965: Calculations of cumulus vertical draft velocities in hurricanes from aircraft observations. J. Appl. Meteor., 4, 463-474.

Gray, W. M., 1967: The mutual variation of wind, shear and baroclinicity in the cumulus convective atmosphere. Mon. Wea. Rev., 95, 55-74.

Gray, W. M., 1979: Hurricanes, their formation, structure and likely role in the tropical circulation. Meteor. over the Tropical Oceans, Roy. Meteor. Soc., Glaisher House, Bracknell, Berkshire, RG12 1Bx, 155-218.

Gray, W. M., 1981: Recent advances in tropical cyclone research from rawinsonde composite analysis. WMO Programme on Research in Tropical Meteorology. This report was prepared at the request of the WMO Commission for Atmospheric Science, Geneva, Switzerland, 407 pp.

Gray, W. M., and D. J. Shea, 1973: The hurricane's inner core region. II. Thermal stability and dynamic characteristics. J. Atmos. Sci., 30, 1565-1576.

Grocott, D. F., 1963: Doppler correction for surface movement. J. of Instrument Navigation, 16, 57-63.

Hawkins, H. F., 1962: Vertical wind profiles in hurricanes. NHRP Report No. 55, 16 pp.

Hawkins, H. F., 1971: Comparison of results of the Hurricane Debbie (1969) modification experiments with those from Rosenthal's numerical model simulation experiments. Mon. Wea. Rev., 99, 427-434.

Hawkins, H. F., and S. M. Imbembo, 1976: The structure of a small intense hurricane - Inez 1966. Mon. Wea. Rev., 104, 418-442.

Hawkins, H. F., and D. T. Rubsam, 1968a: Hurricane Hilda, 1964. I. Genesis, as revealed by satellite photographs conventional and aircraft data. Mon. Wea. Rev., 96, 428-452.

Hawkins, H. F., and D. T. Rubsam, 1968b: Hurricane Hilda, 1964. II. Structure and budgets of the hurricane on October 1, 1984. _Mon. Wea. Rev._, 96, 617-636.

Henderson, R. S., 1978: USAF aerial weather reconnaissance using the Lockheed WC-130 aircraft. _Bull. Amer. Meteor. Soc._, 59, 1136-1143.

Hoecker, W., and G. Brier, 1970: Measurement of hurricane eye diameter by land-based and airborne radar. Air Resources Lab, NOAA.

Holland, G. J., 1980: An analytical model of the wind and pressure profiles in hurricanes. _Mon. Wea. Rev._, 108, 8, 1212-1218.

Holland, G. J., and R. T. Merrill, 1984: On the dynamics of tropical cyclone structural changes. _Quart. J. Meteor. Soc._, 110, 723-745.

Holliday, C. R., and A. H. Thompson, 1979: Climatological characteristics of rapidly intensifying typhoons. _Mon. Wea. Rev._, 107, 1022-1034.

Hoose, H. M., and J. A. Colon, 1970: Some aspects of the radar structure of Hurricane Beulah on September 9, 1967. _Mon. Wea. Rev._, 98, 529-533.

Hughes, L. A., 1952: On the low level wind structure of tropical cyclones, _J. Meteor._, 9, 422-428.

Huntley, J. E., and J. W. Diercks, 1981: The occurrence of vertical tilt in tropical cyclones. _Mon. Wea. Rev._, 109, 1689-1700.

Izawa, T., 1964: On the mean wind structure of typhoons. Japan Typhoon Research Lab. Tech. Note No. 2, 45 pp.

Joint Typhoon Warning Center (JTWC), 1980: Annual tropical cyclone report. US Naval Oceanography Command Center, Joint Typhoon Warning Center, COMNAVMARIANAS Box 17, FPO San Francisco, 96630, NTIS AD A094668, 185 pp.

Joint Typhoon Warning Center (JTWC), 1981: Annual tropical cyclone report. US Naval Oceanography Command Center, Joint Typhoon Warning Center, COMNAVMARIANAS Box 17, FPO San Francisco, 96630, NTIS AD A112002, 194 pp.

Joint Typhoon Warning Center (JTWC), 1982: Annual tropical cyclone report. US Naval Oceanography Command Center, Joint Typhoon Warning Center, COMNAVMARIANAS Box 17, FPO San Francisco, 96630, NTIS AD A124860, 236 pp.

Joint Typhoon Warning Center (JTWC), 1984: Annual tropical cyclone report. US Naval Oceanography Command Center, Joint Typhoon Warning Center, COMNAVMARIANAS Box 17, FPO San Francisco, 96630, 219 pp.

Jordan, C. L., 1961: Marked changes in the characteristics of the eye of intense typhoons between the deepening and filling stages. J. Meteor., 15, 779-789.

Jordan, C. L., D. A. Hurt and C. A. Lowry, 1960: On the structure of hurriane Daisy of 27 August 1958. J. Meteor., 17, 337-348.

Jorgensen, D. P., 1984a: Mesoscale and convective scale characteristics of mature hurricanes. I. General observations by research aircraft. J. Atmos. Sci., 41, 1268-1285.

Jorgensen, D. P., 1984b: Mesoscale and convective scale characteristics of mature hurricanes II. Inner core structure of hurricane Allen (1980), J. Atmos. Sci., 41, 1287-1311.

LaSeur, N. E., and H. F. Hawkins, 1963: An analysis of hurricane Cleo (1958) based on data from research reconnaissance aircraft. Mon. Wea. Rev., 91, 694-709.

Malkus, J. S., 1955: On the structure and maintenance of the mature hurricane eye. J. Meteor., 15, 337-349.

Malkus, J. S., and H. Riehl, 1960: On the dynamics and energy transformations in steady-state hurricanes. Tellus, 12, 1-20.

Merrill, R. T., 1984: A comparison of large and small tropical cyclones. Mon. Wea. Rev., 112, 1408-1418.

Miller, B. I., 1957: On the maximum intensity of hurricanes, NHRP Report No. 14, 19 pp.

Miller, B. I., 1958: The three dimensional wind structure around a tropical cyclone. NHRP Report 15, 41 pp.

Miller, B. I., 1962: On the momentum and energy balance of Hurricane Helene (1958). NHRP Report No. 53, 19 pp.

Powell, M. D., 1982: The transition of the Hurricane Frederick boundary-layer wind field from the open Gulf of Mexico to landfall Mon. Wea. Rev., 110, 1912-1932.

Riehl, H., 1961: Some relations between wind and thermal structure of steady-state hurricanes. J. Atmos. Sci., 20, 276-287.

Riehl, H., and J. Malkus, 1961: Some aspects of hurricane Daisy, 1958. Tellus, 13, 181-213.

Schubert, W. H., and J. Hack, 1982: Inertial stability and tropical cyclone development. J. Atmos. Sci., 39, 1687-1697.

Shea, D. J., and W. M. Gray, 1973: The hurricane's inner core region. I. Symmetric and asymmetric structure. J. Atmos. Sci., 30, 1544-1564.

Shea, D. J., and W. M. Gray, 1976: Data summary of NOAA's hurricane inner-core radial leg flight penetrations 1957-1967, and 1969. Dept. of Atmos. Sci. Paper No. 257, Colo. State Univ., Ft. Collins, CO, 220 pp.

Sheets, R. C., 1967a: On the structure of hurricane Janice (1958). NHRL Report No. 76, 38 pp.

Sheets, R. C., 1967b: On the structure of hurricane Ella (1962). NHRL Report No. 77, 33 pp.

Sheets, R. C., 1968: On the structure of hurricane Dora (1964). NHRL Report No. 83, 64 pp.

Simiu, E., and R. H. Scanlan, 1978: Wind Effects on Structures. Wiley-Interscience, 458 pp.

Simpson, R. H., 1952: Exploring the eye of typhoon Marge, 1951. Bull. Amer. Meteor. Soc., 27, 324-327.

Sugg, A. L., and J. M. Pelissier, 1968: The hurricane season of 1967. Mon. Wea. Rev., 96, 242-250.

Weatherford, C., 1985: Tropical cyclone variability inside 2.5° latitude radius. Paper presented at the 16th Technical Conference on Hurricanes and Tropical Meteorology, AMS, May 14-17, Houston, TX, 62-63.

Weatherford, C., and W. M. Gray, 1984: Relating typhoon intensity to outer $1^{\circ}-3^{\circ}$ radius circulation as measured by reconnaissance aircraft. Paper presented at the 15th Technical Conference on Hurricanes and Tropical Meteorology, AMS, Miami, FL, 238-242.

Willoughby, H. E., J. A. Clos and M. G. Shoreibah, 1982: Concentric eye walls, secondary wind maxima, and the evolution of the hurricane vortex. J. Atmos. Sci., 39 395-411.

W. M. GRAY'S FEDERALLY SUPPORTED RESEARCH PROJECT REPORTS SINCE 1967

CSU Dept. of Atmos. Sci. Report No.	Report Title, Author, Date, Agency Support
104	The Mutual Variation of Wind, Shear and Baroclinicity in the Cumulus Convective Atmosphere of the Hurricane (69 pp.). W. M. Gray. February 1967. NSF Support.
114	Global View of the Origin of Tropical Disturbances and Storms (105 pp.). W. M. Gray. October 1967. NSF Support.
116	A Statistical Study of the Frictional Wind Veering in the Planetary Boundary Layer (57 pp.). B. Mendenhall. December 1967. NSF and ESSA Support.
124	Investigation of the Importance of Cumulus Convection and Ventilation in Early Tropical Storm Development (88 pp.). R. Lopez. June 1968. ESSA Satellite Lab. Support.
Unnumbered	Role of Angular Momentum Transports in Tropical Storm Dissipation over Tropical Oceans (46 pp.). R. F. Wachtmann. December 1968. NSF and ESSA Support.
Unnumbered	Monthly Climatological Wind Fields Associated with Tropical Storm Genesis in the West Indies (34 pp.). J. W. Sartor. December 1968. NSF Support.
140	Characteristics of the Tornado Environment as Deduced from Proximity Soundings (55 pp.). T. G. Wills. June 1969. NOAA and NSF Support.
161	Statistical Analysis of Trade Wind Cloud Clusters in the Western North Pacific (80 pp.). K. Williams. June 1970. ESSA Satellite Lab. Support.
---	A Climatology of Tropical Cyclones and Disturbances of the Western Pacific with a Suggested Theory for Their Genesis/ Maintenance (225 pp.). W. M. Gray. NAVWEARSCHFAC Tech. Paper No. 19-70. November 1970. (Available from US Navy, Monterey, CA). US Navy Support.
179	A diagnostic Study of the Planetary Boundary Layer over the Oceans (95 pp.). W. M. Gray. February 1972. Navy and NSF Support.
182	The Structure and Dynamics of the Hurricane's Inner Core Area (105 pp.). D. J. Shea. April 1972. NOAA and NSF Support.

CSU Dept. of Atmos. Sci. Report No.	Report Title, Author, Date, Agency Support
188	Cumulus Convection and Larger-scale Circulations, Part I: A Parametric Model of Cumulus Convection (100 pp.). R. E. Lopez. June 1972. NSF Support.
189	Cumulus Convection and Larger-scale Circulations, Part II: Cumulus and Meso-scale Interactions (63 pp.). R. E. Lopez. June 1972. NSF Support.
190	Cumulus Convection and Larger-scale Circulations, Part III: Broadscale and Meso-scale Considerations (80 pp.). W. M. Gray. July 1972. NOAA-NESS Support.
195	Characteristics of Carbon Black Dust as a Tropospheric Heat Source for Weather Modification (55 pp.). W. M. Frank. January 1973. NSF Support.
196	Feasibility of Beneficial Hurricane Modification by Carbon Black Seeding (130 pp.). W. M. Gray. April 1973. NOAA Support.
199	Variability of Planetary Boundary Layer Winds (157 pp.). L. R. Hoxit. May 1973. NSF Support.
200	Hurricane Spawned Tornadoes (57 pp.). D. J. Novlan. May 1973. NOAA and NSF Support.
212	A Study of Tornado Proximity Data and an Observationally Derived Model of Tornado Genesis (101 pp.). R. Maddox. November 1973. NOAA Support.
219	Analysis of Satellite Observed Tropical Cloud Clusters (91 pp.). E. Ruprecht and W. M. Gray. May 1974. NOAA/NESS Support.
224	Precipitation Characteristics in the Northeast Brazil Dry Region (56 pp.). R. P. L. Ramos. May 1974. NSF Support.
225	Weather Modification through Carbon Dust Absorption of Solar Energy (190 pp.). W. M. Gray, W. M. Frank, M. L. Corrin, and C. A. Stokes. July 1974.
234	Tropical Cyclone Genesis (121 pp.). W. M. Gray. March 1975. NSF Support.

CSU Dept. of Atmos. Sci. Report No.	Report Title, Author, Date, Agency Support
---	Tropical Cyclone Genesis in the Western North Pacific (66 pp.). W. M. Gray. March 1975. US Navy Environmental Prediction Research Facility Report. Tech. Paper No. 16-75. (Available from the US Navy, Monterey, CA). Navy Support.
241	Tropical Cyclone Motion and Surrounding Parameter Relationships (105 pp.). J. E. George. December 1975. NOAA Support.
243	Diurnal Variation of Oceanic Deep Cumulus Convection. Paper I: Observational Evidence, Paper II: Physical Hypothesis (106 pp.). R. W. Jacobson, Jr. and W. M. Gray. February 1976. NOAA-NESS Support.
257	Data Summary of NOAA's Hurricanes Inner-Core Radial Leg Flight Penetrations 1957-1967, and 1969 (245 pp.). W. M. Gray and D. J. Shea. October 1976. NSF and NOAA Support.
258	The Structure and Energetics of the Tropical Cyclone (180 pp.). W. M. Frank. October 1976. NOAA-NHEML, NOAA-NESS and NSF Support.
259	Typhoon Genesis and Pre-typhoon Cloud Clusters (79 pp.). R. M. Zehr. November 1976. NSF Support.
Unnumbered	Severe Thunderstorm Wind Gusts (81 pp.). G. W. Walters. December 1976. NSF Support.
262	Diurnal Variation of the Tropospheric Energy Budget (141 pp.). G. S. Foltz. November 1976. NSF Support.
274	Comparison of Developing and Non-developing Tropical Disturbances (81 pp.). S. L. Erickson. July 1977. US Army Support.
---	Tropical Cyclone Research by Data Compositing (79 pp.). W. M. Gray and W. M. Frank. July 1977. US Navy Environmental Prediction Research Facility Report. Tech. Paper No. 77-01. (Available from the US Navy, Monterey, CA). Navy Support.
277	Tropical Cyclone Cloud and Intensity Relationships (154 pp.). C. P. Arnold. November 1977. US Army and NHEML Support.
297	Diagnostic Analyses of the GATE A/B-scale Area at Individual Time Periods (102 pp.). W. M. Frank. November 1978. NSF Support.

CSU Dept. of Atmos. Sci. Report No.	Report Title, Author, Date, Agency Support
298	Diurnal Variability in the GATE Region (80 pp.). J. M. Dewart. November 1978. NSF Support.
299	Mass Divergence in Tropical Weather Systems, Paper I: Diurnal Variation; Paper II: Large-scale Controls on Convection (109 pp.). J. L. McBride and W. M. Gray. November 1978. NOAA-NHEML Support.
---	New Results of Tropical Cyclone Research from Observational Analysis (108 pp.). W. M. Gray and W. M. Frank. June 1978. US Navy Environmental Prediction Research Facility Report. Tech. Paper No. 78-01. (Available from the US Navy, Monterey, CA). Navy Support.
305	Convection Induced Temperature Change in GATE (128 pp.). P. G. Grube. February 1979. NSF Support.
308	Observational Analysis of Tropical Cyclone Formation (230 pp.). J. L. McBride. April 1979. NOAA-NHEML, NSF and NEPRF Support.
---	Tropical Cyclone Origin, Movement and Intensity Characteristics Based on Data Compositing Techniques (124 pp.). W. M. Gray. August 1979. US Navy Environmental Prediction Research Facility Report. Tech. Paper No. CR-79-06. (Available from the US Navy, Monterey, CA). Navy Support.
---	Further Analysis of Tropical Cyclone Characteristics from Rawinsonde Compositing Techniques (129 pp.). W. M. Gray. March 1981. US Navy Environmental Prediction Research Facility Report. Tech. Paper No. CR-81-02. (Available from the US Navy, Monterey, CA). Navy Support.
333	Tropical Cyclone Intensity Change - A Quantitative Forecasting Scheme. K. M. Dropco. May 1981. NOAA Support.
---	Recent Advances in Tropical Cyclone Research from Rawinsonde Composite Analysis (407 pp.). WMO Publication. W. M. Gray. 1981.
340	The Role of the General Circulation in Tropical Cyclone Genesis (230 pp.). G. Love. April 1982. NSF Support.
341	Cumulus Momentum Transports in Tropical Cyclones (78 pp.). C. S. Lee. May 1982. ONR Support.

CSU Dept. of Atmos. Sci. Report No.	Report Title, Author, Date, Agency Support
343	Tropical Cyclone Movement and Surrounding Flow Relationships (68 pp.). J. C. L. Chan and W. M. Gray. May 1982. ONR Support.
346	Environmental Circulations Associated with Tropical Cyclones Experiencing Fast, Slow and Looping Motions (273 pp.). J. Xu and W. M. Gray. May 1982. NOAA and NSF Support.
348	Tropical Cyclone Motion: Environmental Interaction Plus a Beta Effect (47 pp.). G. J. Holland. May 1982. ONR Support.
---	Tropical Cyclone and Related Meteorological Data Sets Available at CSU and Their Utilization (186 pp.). W. M. Gray, E. Buzzell, G. Burton and Other Project Personnel. February 1982. NSF, ONR, NOAA, and NEPRF Support.
352	A Comparison of Large and Small Tropical Cyclones (75 pp.). R. T. Merrill. July 1982. NOAA and NSF Support.
358	On the Physical Processes Responsible for Tropical Cyclone Motion (200 pp.). Johnny C. L. Chan. November 1982. NSF, NOAA/NHRL and NEPRF Support.
363	Tropical Cyclones in the Australian/Southwest Pacific Region (264 pp.). Greg J. Holland. March 1983. NSF, NOAA/NHRL and Australian Government Support.
370	Atlantic Seasonal Hurricane Frequency, Part I: El Nino and 30 mb QBO Influences; Part II: Forecasting Its Variability (105 pp.). W. M. Gray. July 1983. NSF Support.
379	A Statistical Method for One- to Three-Day Tropical Cyclone Track Prediction (201 pp). Clifford R. Matsumoto. December, 1984. NSF/NOAA and NEPRF support.
---	Varying Structure and Intensity Change Characteristics of Four Western North Pacific Tropical Cyclones. (100 pp.). Cecilia A. Askue and W. M. Gray. October 1984. US Navy Environmental Prediction Research Facility Report No. CR 84-08. (Available from the US Navy, Monterey, CA). Navy Support.

CSU Dept. of
Atmos. Sci.
<u>Report No.</u>   <u>Report Title, Author, Date, Agency Support</u>

---   Characteristics of North Indian Ocean Tropical Cyclone
             Activity. (108 pp.). Cheng-Shang Lee and W. M. Gray.
             December 1984. US Navy Environmental Prediction Research
             Facility Report No. CR 84-11. (Available from the US
             Navy, Monterey, CA). Navy Support.

391   Typhoon Structural Variability. (77 pp.). Candis L.
             Weatherford. October, 1985. NSF/NOAA Support.

             Tropical cyclone structure and intensity change (290 pp.).
             Edwin Nunez. NSF Support.

             Global View of the Upper Level Outflow Patterns Associated
             with Tropical Cyclone Intensity Change During FGGE.
             L. Chen and W. Gray, 150 pp. NASA support.

BIBLIOGRAPHIC DATA SHEET	1. Report No. ATS-391	2.	3. Recipient's Accession No.
4. Title and Subtitle Typhoon Structural Variability			5. Report Date October, 1985
			6.
7. Author(s) Candis L. Weatherford			8. Performing Organization Rept. No. ATS-391
9. Performing Organization Name and Address Atmospheric Science Department Colorado State University Fort Collins, Colorado 80523			10. Project/Task/Work Unit No.
			11. Contract/Grant No. ATM 8419116
12. Sponsoring Organization Name and Address NSF/NOAA Grant No. ATM 8419116 National Science Foundation 18th and G Streets, N.W., Washington, D.C. 20550			13. Type of Report & Period Covered Project Report
			14.

15. Supplementary Notes

16. Abstracts

This paper describes the varying structure of the tropical cyclone wind profile in terms of its core intensity, outer strength, and size where core intensity is defined by the tropical cyclone's minimum central sea-level pressure, outer strength is an average tangential wind speed from 60 to 150 n mi (111-278 km), and size measures the radial extent of 30-kt and 50-kt surface winds. Analysis was performed on 700 mb aircraft data from over 500 reconnaissance missions into 66 tropical cyclones of the northwestern Pacific. All these cyclones were of typhoon intensity ($V_{max} >> 65$ knots) sometime during their lifecycle. This data set is uniquely suited to fill the dual needs of: 1) providing inner wind profile information out to $4°$ radius, thus allowing the cyclone's strength to be measured, and 2) being able to sample the entire life cycle of the tropical cyclone from depression through supertyphoon stages. The focus of this study is on the outer strength region.

17. Key Words and Document Analysis. 17a. Descriptors

Typhoons
Tropical Cyclones
Typhoon Intensity

17b. Identifiers/Open-Ended Terms

17c. COSATI Field/Group

18. Availability Statement	19. Security Class (This Report) UNCLASSIFIED	21. No. of Pages 77
	20. Security Class (This Page) UNCLASSIFIED	22. Price

END

DTIC

5—86